Title: MAPK/ERK Activation in Macrophages Promotes *Leishmania* Internalization and Pathogenesis

Running title: ERK1/2 facilitates *Leishmania* internalization

Authors: Umaru Barrie[1, 2], Katherine Floyd[1, #], Arani Datta[1], and Dawn M. Wetzel[1, 3*]

Affiliations: [1]Department of Pediatrics, University of Texas Southwestern Medical Center, 5323 Harry Hines Blvd, Dallas, Texas, 75390, United States; [2]Medical Scientist Training Program, University of Texas Southwestern Medical Center, 5323 Harry Hines Blvd, Dallas, Texas, 75390, United States; [3]Department of Biochemistry, University of Texas Southwestern Medical Center, 5323 Harry Hines Blvd, Dallas, Texas, 75390, United States.

*Corresponding author: Dawn M. Wetzel, M.D., Ph.D.
Departments of Pediatrics (Infectious Diseases) and Biochemistry
The University of Texas Southwestern Medical Center, Dallas, TX 75019
Phone: 214-645-9510; Email: Dawn.Wetzel@UTSouthwestern.edu

[#]**Current address:** Department of Internal Medicine and Molecular Microbiology, Washington University School of Medicine, 660 S Euclid Ave, St. Louis, MO 63110, United States

Author contributions: U.B. and D.M.W. designed and performed experiments, analyzed data, and wrote the manuscript. K.F. conducted experiments, assisted with data analysis, and edited the manuscript. A.D. helped to design and perform experiments, analyzed data, and edited the manuscript.

This file includes:

Abstract word count: 224

Lay summary word count: 142

Manuscript word count: 6602

Number of references: 63

Number of figures: 6

Number of tables: 2

Supplemental figures: 4

Supplemental tables: 3

ABSTRACT: The obligate intracellular protozoan parasite *Leishmania* binds several host cell receptors to trigger its uptake by phagocytic cells, ultimately resulting in visceral or cutaneous leishmaniasis. After *Leishmania* engages receptors on macrophages and other phagocytes, a series of signaling pathways in the host cell are activated during its internalization, which are critical for establishment and persistence of *Leishmania* infection. Thus, preventing *Leishmania* internalization by phagocytes could be a novel therapeutic strategy for leishmaniasis. However, the host cellular machinery that mediates promastigote and amastigote uptake is not well understood. Here, using small molecule inhibitors of Mitogen-activated protein kinases/Extracellular signal regulated kinases (MAPK/ERK), we demonstrate that ERK1/2 mediates *Leishmania amazonensis* uptake and (to a lesser extent) phagocytosis of beads by macrophages. We find that inhibition of MEK1/2 or ERK1/2 leads to inefficient amastigote uptake by macrophages. Moreover, using inhibitors and primary macrophages lacking spleen tyrosine kinase (SYK) or Abl family kinases, we show that SYK and Abl family kinases mediate Raf, MEK, and ERK1/2 activity and are necessary for efficient uptake. Finally, we demonstrate that trametinib, a MEK1/2 inhibitor used clinically to treat certain cancers, significantly reduces disease severity and parasite burden in *Leishmania*-infected mice, even if it is started significantly after lesions develop. Our results show that maximal *Leishmania* infection requires MAPK/ERK and highlight the potential for MAPK/ERK-mediated signaling pathways to be novel therapeutic targets for leishmaniasis.

Keywords: *Leishmania*, kinase, MAPK/ERK, parasite, macrophage

Abbreviations: BCA, Bicinchoninic acid; BMDM, bone marrow-derived macrophages; CC, cytotoxic concentration; CR3, complement receptor 3; FcγR, Fc gamma Receptor; h, hour; IC, inhibitory concentration; IL, Interleukin; INFγ, Interferon gamma; Mϕ, macrophage; m, minutes; MAPK/ERK, Mitogen-activated protein kinases/Extracellular signal regulated kinases; PKC, Protein Kinase C; PVDF, polyvinylidene difluoride; RAF, Rapidly Accelerated Fibrosarcoma; RIPA, radioimmunoprecipitation assay; p-, phosphorylated; PMA, Phorbol 12-myristate 13-acetate; SD, standard deviation; SFK, Src family kinases; SYK, spleen tyrosine kinase; TNF, Tumor Necrosis Factor

Lay summary: *Leishmania* is a single-celled parasite that causes skin ulcers or a disseminated disease in humans. Our goal is to identify new drugs to treat *Leishmania* infection. *Leishmania* must live inside human immune cells to cause disease. If *Leishmania* is not able to enter human immune cells, it dies. Our studies demonstrate how *Leishmania* infection permits a set of proteins called MAP kinases to pass signals from one protein to the next within mammalian immune cells. The resulting signals allow *Leishmania* to enter into these immune cells and survive within its host. Importantly, trametinib, a drug that prevents these signals from MAP kinases, decreases the development of skin ulcers when it is given to mice that are infected with *Leishmania*. Our findings suggest that

84 leishmaniasis could be treated with drugs that act on kinases found in humans

85 rather than the parasites themselves.

86

87 **One sentence summary**: An Abl2-SYK-Raf-MEK-ERK pathway facilitates

88 *Leishmania* uptake by phagocytic cells and promotes disease severity in

89 *Leishmania*-infected mice.

90

1. INTRODUCTION

Leishmania spp. are obligate intracellular, protozoan parasites spread by the sand fly vector [1], causing leishmaniasis, a group of diseases ranging from self-healing cutaneous ulcers [2] to deadly disseminated visceral disease [3]. Leishmaniasis represents a major global health problem, since over 12 million people currently suffer from this disease. Approximately 2 million people are newly infected by *Leishmania* spp. annually [4]. Moreover, over 350 million people in 98 countries worldwide are at risk of developing leishmaniasis [4, 5], and the disease is now spreading into previously non-endemic areas, including the United States [6, 7]. *Leishmania*, particularly the species causing cutaneous disease, are understudied, and current treatments are few, expensive, poorly effective, and toxic. Resistance is also emerging [8-11]. Thus, identifying new drugs with novel mechanisms of action that circumvent resistance mechanisms is an urgent priority for effective drug development.

When an infected sand fly encounters its host, *Leishmania* promastigotes must be internalized by phagocytic cells such as macrophages (Mϕ) to persist in the host [12, 13]. This process is then repeated as the mammalian life cycle stage, the amastigote, replicates and spreads to other phagocytic cells to cause pathogenesis [14]. Amastigotes that do not enter phagocytic cells are thought to be cleared by the host immune system and/or die from lack of essential nutrients [14]. Major advancements have been made in understanding the immunomodulatory events involved in the pathogenesis of leishmaniasis.

114 However, little is known about the basic molecular events underlying the
115 pathogenesis, especially the host cellular signaling pathways, which facilitate the
116 uptake of *Leishmania* by Mϕs and other phagocytes.
117
118 Based on prior studies, the Fcγ classes of receptors (FcγR) are the primary
119 receptors on the host cell surface that permit amastigote uptake [14], and the
120 complement receptor CR3 is the primary mediator of promastigote uptake [15].
121 Our previous studies have identified the Src [16] family kinases (SFK, and
122 specifically Hck, Fgr, and Lyn), Abl1 (Abl) and Abl2 (Arg) [17] kinases, and
123 Spleen Tyrosine Kinase (SYK) [18] as major protein families involved in
124 phagocytosis and *Leishmania* uptake. Specifically, we have demonstrated that
125 Abl facilitates complement-mediated phagocytosis, and Arg enhances
126 immunoglobulin/ FcγR-mediated phagocytosis [16, 17]. Modulation of these
127 kinases via genetic manipulation or small molecule inhibitors abrogates *L.*
128 *amazonensis* internalization by Mϕs, and thus limits disease progression in mice
129 [16, 17]. However, our studies also indicate that these kinases have a limited role
130 in the host's immune response to *Leishmania* or parasite clearance [16, 17]. A
131 drug that simultaneously decreases parasite uptake and promotes host-
132 advantageous immunological responses could provide reductions in infection and
133 disease burden. Host-cell active agents also could be used to combat other
134 intracellular pathogens that employ similar uptake mechanisms.
135

136 Exactly how SFK, Abl family kinases, and SYK would regulate the events that
137 occur during *Leishmania* uptake and phagocytosis has not been fully established.
138 Others and we have demonstrated that CrkII is activated after signals have been
139 relayed from SFK to Arg to SYK, leading to actin-rich phagocytic cup formation
140 and pathogen uptake [16-19]. Interestingly, studies have been published
141 primarily in cancer model systems indicating that SFK [20], Abl family kinases
142 [20], and SYK [21, 22] also can activate MAPK/ERK signaling. MAPK/ERK are
143 known to directly phosphorylate cytoplasmic or nuclear proteins, including
144 transcription factors, that control several fundamental cellular processes from
145 proliferation and differentiation to innate and adaptive immune responses [23-25].
146 In addition, Phorbol 12-myristate 13-acetate (PMA) is known to activate
147 MAPK/ERK through protein kinase C (PKC) [26].
148
149 It is not clear whether MAPK/ERK signaling would mediate the uptake of
150 *Leishmania* parasites by phagocytes. Research on *Plasmodium* indicated that
151 inhibiting MEK1/2, which is upstream of ERK1/2, affects both adaptive and innate
152 immune responses, which limits parasitemia and prevents pathogenesis [27].
153 Previous studies have also shown that MAPK/ERK signaling modulates the
154 immune response to *Leishmania* infection to favor chronic infection, where
155 subversion of MAPK/ERK signaling leads to parasite survival inside phagocytic
156 cells [28-32]. Correspondingly, limiting MAPK activity using the older-generation
157 MAPK inhibitors PD98059 or U0126 has been shown to enhance *L.*
158 *amazonensis* killing by activating reactive oxygen species (ROS) and repressing

159 IL-10 production [33-36]. These results implicate ERK1/2 phosphorylation as a
160 mechanism through which the parasite promotes persistence and subverts the
161 immune response [33]. However, experiments characterizing the role of
162 MAPK/ERK signaling during parasite uptake by Mϕ have not been conducted.
163
164 Here, we uncover an additional role for MAPK/ERK during *Leishmania*
165 internalization by phagocytes. We show that Raf-1, MEK1/2, and ERK1/2 activity are
166 necessary for efficient uptake of amastigotes. Host MAPK/ERK is activated by Arg
167 and SYK to facilitate this process. In combination with prior results [16, 17, 33], our
168 molecular studies elucidate an FcγR-SFK-Arg-SYK-Raf-MEK-ERK signaling relay as
169 a major pathway involved in establishment of leishmaniasis by facilitating parasite
170 uptake. In addition, using a mouse model, we establish that trametinib, a selective
171 MEK inhibitor that is clinically approved to treat cancer, decreases footpad swelling
172 and parasite burden in cutaneous leishmaniasis, even if it is started significantly after
173 lesions are apparent. Our experiments highlight MAPK/ERK inhibitors as potential
174 treatment modalities for this devastating disease.
175

176 **2. MATERIALS AND METHODS:**

177 **2.1 Mice.** C57BL/6 mice were procured from Jackson Laboratory (Bar Harbor, ME).
178 *Syk*$^{flox/flox}$ *Cre*$^{+}$ and *Arg*$^{-/-}$*Abl*$^{flox/flox}$ *LysM Cre*$^{+}$ mice are either on a pure C57BL/6
179 background (SYK) [18] or have been backcrossed to C57BL/6 mice at least 5 times
180 (Abl/Arg) [16], [17]. All the experiments involving knockout mice were conducted with
181 WT littermates to ensure control for their genetic background. The Institutional
182 Animal Care and Use Committee at University of Texas Southwestern Medical
183 Center provided approval for all experimental protocols.
184

185 **2.2 Mammalian cell culture.** RAW 264.7 cells (ATCC, Manassas, VA) were
186 cultured in Dulbecco's modified Eagle's medium (DMEM) plus 10% endotoxin-free,
187 heat-inactivated, fetal bovine serum (FBS) (GeminiBio, Sacramento, CA) and 1%
188 penicillin–streptomycin as described previously [16]. FBS was checked for LPS
189 contamination using a highly sensitive Pierce™ Chromogenic Endotoxin Quant Kit
190 (Thermo Scientific, Cat No. A39552), and was found to be endotoxin negative (< 0.1
191 EU/ml). For experiments with bone marrow-derived Mϕs (BMDM), cells were
192 obtained from the humeri, tibias, and femurs of *WT, Syk*$^{flox/flox}$ *Cre*$^{+}$, or *Arg*$^{-/-}$*Abl*$^{flox/flox}$
193 *LysM-Cre*$^{+}$ mice. They were differentiated to *WT, Syk*$^{flox/flox}$ *Cre*$^{+}$, or *Arg*$^{-/-}$*Abl*$^{flox/flox}$
194 *LysM-Cre*$^{+}$ BMDM by culturing them in DMEM, 10% FBS, and 20% L929 cell
195 supernatant over 7 days. Differentiation to Mϕ was confirmed [17] and samples were
196 screened for *Mycoplasma* contamination [37].
197

198 **2.3 Parasite culture.** *L. amazonensis* promastigotes (strain IFLA/BR/67/PH8,
199 provided by Norma W. Andrews, University of Maryland, College Park, MD) were
200 maintained at 26°C in Schneider's Drosophila medium (Sigma, S9895, St. Louis,
201 MO) plus 15% FBS and 1% penicillin–streptomycin [16, 17]. *L. amazonensis*
202 amastigotes were grown axenically at 32°C in Schneider's Drosophila medium at
203 pH 5.5, plus 20% FBS, 1% penicillin–streptomycin, 0.1% hemin (25 mg/mL in
204 50% triethanolamine), 10 mM adenine, 5 mM L-glutamine, 0.25% glucose, 0.5%
205 trypticase, and 40 mM sodium succinate (all from Sigma) [16, 17]. For uptake
206 (internalization of amastigotes and promastigotes) assays, promastigotes were
207 incubated for 7 days to maximize infective metacyclics (*i.e.*, those isolated
208 through a step Percoll gradient; Sigma). Amastigotes typically were grown
209 axenically for 5 days prior to use [17]. To assess for amastigote growth and
210 replication defects during incubation in MEK/ERK activators or inhibitors, medium
211 containing 10 μM trametinib (Selleck Chemicals, Houston, TX), PMA (Selleck
212 Chemicals), or 0.1% dimethyl sulfoxide (DMSO, Sigma) was used. To ensure
213 infectivity, parasites were periodically passed in C57/BL6 mice prior to isolation
214 of amastigotes from footpad lesions.
215
216 For some experiments, a transgenic stable mNeonGreen expressing line of *L.*
217 *amazonensis* parasites (*L. amazonensis*-mNeon), containing a marker for
218 hygromycin resistance, was generated [18]. *L. amazonensis*-mNeon
219 promastigotes and amastigotes were maintained as above, but the media was
220 supplemented with 100 μg/mL hygromycin (Sigma). *L. amazonensis* virulence

221 was maintained by passage in C57BL/6 mice [17]. *L. amazonensis*-mNeonGreen
222 parasites were detected with an excitation wavelength of 490–494 nm and
223 emission of 515 nm.
224
225 **2.4 *Leishmania* uptake assays.** Experiments were adapted and modified as
226 described previously [16, 17]. BMDM (*WT, Syk*$^{flox/flox}$ *Cre*$^{+}$, *Arg*$^{-/-}$*Abl*$^{flox/flox}$ *LysM-Cre*$^{+}$)
227 or RAW 264.7 cells were plated and treated with inhibitors (imatinib [Arg/Abl
228 inhibitor], PD0325901 [MEK1/2 inhibitor], SCH772984 [ERK1/2 inhibitor], trametinib
229 [MEK1/2 inhibitor]) (Selleck Chemicals, Houston, TX), PMA [ERK1/2 activator] or
230 DMSO, where appropriate. Metacyclic promastigotes were incubated in fresh mouse
231 serum for C3bi opsonization, and amastigotes were coated with anti-P8-
232 proteoglycolipid complex (monoclonal antibody IgG1) [18]. Next, samples with RAW
233 264.7 cells or BMDMs were incubated with C3bi-opsonized promastigotes at 10
234 parasites to 1 Mϕ or with IgG-opsonized amastigotes at 10 parasites to 1 Mϕ for 2
235 hours (h), unless otherwise indicated, and fixed with 3% formaldehyde for 20
236 minutes (m). Mouse anti-gp46 antibody was allowed to bind to external
237 promastigotes, whereas mouse anti-P8 antibody was incubated with external
238 amastigotes, as described previously [16, 17]. Samples were then incubated with
239 Alexa-Fluor-568-conjugated donkey anti-mouse-IgG secondary antibody. Any
240 internalized parasite did not receive any antibody tagging and fluoresces green.
241 Conversely, external parasites are visualized in both the red and green channels
242 (orange in a merged image). All antibodies are listed in **Supplemental Table 3**.
243 Thus, this three-color immunofluorescence assay [18] allowed distinguishing of

244 internal (green) and external *L. amazonensis* promastigotes or amastigotes (green +
245 red).
246
247 For quantification, samples were imaged with a BioTek Cytation 5 (Agilent, Santa
248 Clara, CA) confocal imaging reader using a 40x objective lens with automated
249 analysis performed [16]. At least 16 randomly selected fields were automatically
250 visualized per well with each field assessing the number of Mϕs and amastigotes or
251 promastigotes (internalized versus external). The absolute phagocytic index (the
252 number of internalized amastigotes or promastigotes per 100 Mϕs) and adhesion
253 index (the total number of amastigotes or promastigotes per 100 Mϕs) was
254 calculated for each condition. The absolute phagocytic index or adhesion index for
255 DMSO-treated conditions (control) was taken as the maximum value (100%) for
256 each experiment, and the phagocytic index for imatinib, SCH772984, trametinib, or
257 PMA-treated samples was determined and normalized relative to that of the control.
258 Means ± SD were calculated. Each experiment was performed with at least 3
259 biological repeats and contained 3 technical replicates. A one-sample Student's *t*-
260 test or two-way ANOVA was used to determine statistical significance, where
261 appropriate. The representative images shown were visualized using a Biotek
262 Cytation 5 imaging multimode reader. Parasites in representative images were
263 selected from files and linearly processed in Adobe Photoshop CS6 (version 13.0.6).
264 Where applicable, permeabilized samples were labeled with far-red phalloidin
265 (A22287, Thermo Fisher Scientific) at 1:100. For phagocytic cup analysis and
266 representative images, data were collected on a Zeiss LSM 880 inverted confocal

267 Airyscan microscope at 40X (analysis) or 63X (representative images) and
268 processed in Adobe Photoshop 13.0.6 [38]. created via Image J (1.52a,
269 http://imagej.nih.gov/ij) and processed in Adobe Photoshop 13.0.6.
270
271 **2.5 Phagocytosis of beads.** Experiments were adapted and modified as described
272 previously [16, 17]. RAW 264.7 cells were plated at 70% confluence and incubated
273 overnight in serum-free medium. Except where indicated, samples were pre-
274 incubated in medium containing 3.3 μM imatinib, 1 μM SCH772984, 1 μM trametinib,
275 250 nM PMA or 0.1% DMSO for 1-2 h. Next, latex yellow–green 2 μm beads
276 (Sigma) were coated with human IgM (Sigma, Cat. #: I-8260) and incubated in rabbit
277 anti-IgM (Sigma, Cat. #: 270A) for IgG opsonization (confirmed as described
278 previously [17]). Mϕs were incubated with 10–15 beads/ Mϕ for 2 h, unless otherwise
279 stated, at 37°C. They were fixed with 3% formaldehyde for 20 m, blocked using 2%
280 BSA in PBS (no permeabilization), and then incubated with rabbit anti-human IgM
281 and Hoechst 33258 dye (Sigma) to visualize nuclei. Next, samples were incubated
282 with an Alexa-Fluor-568-conjugated goat anti-rabbit-IgG secondary antibody
283 (Invitrogen, Cat.#: A11034). All antibodies are listed in **Supplemental Table 3**. This
284 multi-color immunofluorescence assay [39] allowed distinguishing of internalized
285 (green) and external beads (green + red), similar to described above for internal vs
286 external *L. amazonensis*. Quantification was done as above with a BioTek Cytation 5
287 confocal imaging reader using a 40x objective lens with automated analysis
288 performed by the Cytation 5.
289

290 **2.6 Western Blot**. To analyze protein/phosphoprotein expression, western blotting
291 was performed. Briefly, RAW 264.7 cells or BMDMs from *WT, Syk*$^{flox/flox}$ *Cre*$^{+}$, or
292 *Arg*$^{-/-}$*Abl*$^{flox/flox}$ *LysM-Cre*$^{+}$ mice were incubated overnight in serum-free media (RAW
293 264.7 cells) or L929-free media (BMDM). Experiments were performed at ~70%
294 confluence. Where appropriate, Mϕ were pre-incubated in imatinib, entospletinib,
295 PD0325901, selumetinib, SCH772984, trametinib, PMA or DMSO. IgG-opsonized
296 amastigotes or IgG-opsonized beads were added to adherent starved Mϕs for 30 m,
297 unless otherwise indicated [40], and cells lysed with RIPA extraction buffer and halt
298 protease and phosphatase inhibitor (Thermo Scientific, Cat. #: 78440, Richardson,
299 TX). Protein purity and concentration were addressed using Coomassie Blue
300 staining and BCA assay, respectively, following the manufacturers' protocols. Total
301 proteins were resolved by polyacrylamide gel electrophoresis (12% gels) and
302 transferred to PVDF membranes (BioRad). The membranes were blocked in 5%
303 non-fat dry milk in Tris-buffered saline (TBS) (20 mM Tris at pH 7.6, 150 mM NaCl).
304 The membrane was incubated overnight at 4˚C with the primary antibody in 5% BSA
305 and TBS-T. Next, horseradish peroxidase (HRP)-conjugated anti-mouse secondary
306 antibody (#7076, Cell Signaling Technology) was added at 1:5000 in 5% non-fat dry
307 milk in TBS-T for 1 h. All antibodies are provided in **Supplemental Table 3**.
308 Membranes were incubated in SuperSignal West Pico Chemiluminescent Substrate
309 (Thermo Scientific) for 5 m and visualized by using a phosphorimager (ImageQuant
310 LAS 4000, GE Healthcare). For analysis, relative amounts of phosphorylated
311 proteins were compared to total proteins with ImageJ analysis software
312 (https://imagej.nih.gov/ij); membranes were stripped and reprobed). Each

313 experiment had at least 3 biological replicates. Two-way ANOVA was used for
314 statistical tests.
315
316 **2.7 *Leishmania* animal model.** For the mouse footpad model of cutaneous
317 leishmaniasis, 10 female C57BL/6 mice per group were infected between 6 and 8
318 weeks (w) of age as previously described [16, 17]. Briefly, 1×10^6 metacyclic
319 promastigotes were suspended in PBS and injected subcutaneously in the dorsal
320 side of the right hind foot. For the experiments in Fig 6A-C, mice were provided 2
321 mg/kg body weight of trametinib or drug vehicle (4% DMSO and 1% corn oil) by oral
322 gavage daily starting a w before infection and continuing until the mice were
323 euthanized. Two independent experiments were performed. For the experiments in
324 Fig 6D-F, mice were provided 2 mg/kg body weight of trametinib or drug vehicle by
325 oral gavage daily starting 6 w after infection and continuing until the mice were
326 euthanized. Two independent experiments were performed. Lesion growth was
327 documented with calipers every other w by an investigator who was blinded to
328 condition. The ratio of the infected: uninfected foot size was obtained [41]. ANOVA
329 was used to compare diluent and trametinib-treated mouse groups to swelling at
330 time 0. The number of parasites in lesions was determined by limiting dilution upon
331 termination of the experiment between w 14 to 16 [42].
332
333 Lymph nodes from infected diluent versus trametinib-treated mice were obtained for
334 cytokine and chemokine profiling [42, 43]. Briefly, lymph node cells were incubated
335 in RPMI 1640 (Invitrogen) plus 10% heat-inactivated FBS, 5×10^{-5} M 2-

336 mercaptoethanol (Sigma), and 1% penicillin-streptomycin. Cells were stimulated with
337 promastigote lysates (equivalent to 1×10^6 or 1×10^5 parasites per sample, as
338 indicated) or concanavalin A (ConA) (5 μg/ml; Sigma). Supernatants were harvested
339 at 72 h and the levels of the cytokines and chemokines IL-4, IL-10, IL-12, IL-13, IL-
340 17, IFN-γ, IL-1β, IL-1α, IP-10, MIP-1α (CCL3), MIP-2 (CXCL2), CXCL9, RANTES
341 (CCL5), and MIP-1β (CCL4) were profiled using the custom multiplex Luminex
342 Platform (R&D Systems, Inc, Minneapolis, MN) through the UT Southwestern
343 Microarray Core as described previously [44, 45]. Background cytokine levels were
344 calculated using unstimulated supernatants.
345

346 **3. RESULTS**

347 **3.1 MAPK/ERK signaling in Mϕ facilitates *Leishmania* uptake**

348 To directly test whether the MAPK/ERK pathway mediates *Leishmania* uptake,
349 we first explored the effect of the MEK1/2 inhibitor trametinib on the uptake of *L.*
350 *amazonensis*. We can grow both promastigotes and amastigotes of this species
351 in tissue culture without host cells (*i.e.*, axenic culture), which facilitates our
352 studies of *Leishmania* uptake by Mϕs. Trametinib is a highly selective and potent
353 MEK1/2 inhibitor, with an IC_{50} for the purified kinase ranging from 0.92 nM to 3.4
354 nM in cell-free assays [46, 47]. Trametinib has no effect on the kinase activity of
355 c-Raf, B-Raf, or ERK1/2. We pretreated RAW 264.7 cells, a Mϕ–like cell line, for
356 2 hours (h) with trametinib or imatinib, an Abl/Arg inhibitor with an IC_{50} of 100-500
357 nM in kinase assays [35], as a positive control. We then added *Leishmania* to
358 samples to allow uptake and processed for immunofluorescence microscopy.
359 Visually, trametinib decreased the uptake of IgG-opsonized amastigotes in RAW
360 264.7 cells, comparable to the reductions seen after treatment with imatinib (**Fig.**
361 **1A).** Defects in internalization were quantified by calculating the phagocytic index
362 (PI), or number of internalized parasites per 100 Mϕ, which was lower in
363 trametinib-treated samples (**Fig. 1B**). No differences were seen in the total
364 (external + internal) number of *Leishmania* per 100 RAW 264.7 cells, which is
365 termed an adhesion index, among these conditions (**Fig. 1C**). We performed a
366 titration of trametinib's effects on amastigote uptake, and the maximal reduction
367 in PI was shown at 1 μM trametinib (**Fig. 1D, E**)**.** We also determined that over
368 72 h, the CC_{50} (cytotoxic concentration required to kill 50% of viable cells) for

369 RAW 264.7 cells was greater than our maximum concentration of 2.5 μM.
370 Internalization defects remained even after prolonged incubation in trametinib (up
371 to 240 minutes, m) and were not due to reduced adhesion, as amastigotes
372 continued to be bound to trametinib-treated RAW 264.7 cells at levels
373 indistinguishable from controls (**Fig. 1F, G**). Treating Mϕs with other MAPK/ERK
374 pathway inhibitors [48] such as selumetinib and PD0325901 (MEK1/2 inhibitors),
375 as well as SCH772984 (an ERK1/2 inhibitor), also significantly reduced
376 amastigote uptake without affecting adhesion (**Supplemental Fig. 1A, B**). In
377 addition, we found that treating RAW 264.7 cells with the MEK1/2 inhibitor
378 PD0325901 [49] decreased the internalization of promastigotes to a degree that
379 was comparable to imatinib (**Supplemental Fig. 1C, D**). Next, we characterized
380 growth curves and found that trametinib showed no impact on cell viability and
381 motility of parasites in culture (**Fig. 1H**). Together, these similar results using
382 multiple MAPK/ERK inhibitors establish that targeting MEK1/2 and ERK1/2
383 significantly attenuates internalization of both *L. amazonensis* life cycle stages. In
384 addition, as previously published for MAPK/ERK inhibitors, amastigotes within
385 Mϕs had a ~50% reduction in survival when cultures were treated with trametinib
386 for 72 h (**Supplemental Fig. 1E**).
387

388 **3.2 cRaf, MEK1/2, and ERK1/2 are activated during amastigote uptake**

389 Having established that MAPK/ERK are important for *Leishmania* uptake, we
390 assessed whether kinases in this pathway were activated in host cells during
391 amastigote internalization. Raf-1 (cRaf), MEK1/2, and ERK1/2 are key members of

392 the MAPK/ERK pathway [25, 50]. We thus measured cRaf, MEK1/2, and ERK1/2
393 phosphorylation in RAW 264.7 cells to examine the relative phosphorylation level of
394 each kinase during internalization of amastigotes. Essentially no phosphorylated
395 ERK or ERK was detected in amastigote samples (**Supplemental Fig. 2A**).
396 However, amastigotes potently induced ERK1/2 phosphorylation in Mϕs, with
397 phosphorylation levels increasing by 3 and 4.5-fold at 10 and 30 m post-infection,
398 respectively (**Fig. 2A**). Similarly, MEK1/2 (**Fig. 2B**) and cRaf (**Fig. 2C**) were
399 activated by amastigotes that were entering host cells**.** These data indicate that
400 amastigotes rapidly activate MAPK/ERK in a sustained fashion during their uptake
401 by Mϕs.
402
403 **3.3 PMA rescues MAPK/ERK related uptake defects**
404 PMA is known to activate ERK1/2 through PKC, with an IC_{50} of 11.7 nM against
405 purified kinase [26]. Consistent with this, although PKC activation was seen during
406 the uptake of amastigotes, PMA treatment increased PKC phosphorylation in RAW
407 264.7 cells to 8-fold higher levels (**Fig. 3A, B**). Importantly, 10 μM PMA did not affect
408 growth of amastigotes in culture (**Fig. 3C**), indicating that it does not act directly on
409 *Leishmania*. We next investigated whether PMA affected amastigote internalization.
410 To perform these experiments, and to confirm our prior results from a cell line using
411 primary cells, we isolated bone marrow derived-Mϕs (BMDM) from C57BL/6 mice.
412 PMA-treated BMDM were able to internalize IgG-coated amastigotes at higher levels
413 than DMSO-treated BMDM in a dose-dependent manner, reaching maximal
414 internalization at 2.5 μM PMA (**Fig. 3D-F**). Furthermore, PMA treatment rescued

415 trametinib inhibition of *Leishmania* uptake in BMDM to PI that were indistinguishable
416 from those of DMSO-treated controls (**Fig. 3G, H**). Collectively, our data indicate that
417 ERK1/2 kinase activity is necessary for maximal *Leishmania* uptake.
418
419 **3.4 ERK1/2 is activated by Arg/Abl and SYK during amastigote uptake**
420 Next, we investigated the mechanism by which *L. amazonensis* amastigotes induced
421 ERK1/2 phosphorylation during their uptake. Previous research has shown that Arg
422 facilitates *Leishmania* amastigote uptake downstream of SFK [16]. In addition,
423 inhibition of SYK, a tyrosine kinase implicated in FcγR immunoglobulin-mediated
424 signaling [18, 33, 51, 52] reduces ERK1/2 activation in a dose-dependent manner in
425 other systems [18, 33]. To test for roles for these kinases, small molecule inhibitors
426 (imatinib, entospletinib [IC_{50} for activity against purified SYK = 7.7 nM] [18],
427 SCH772984, trametinib), and PMA were added to RAW 264.7 cells before infection
428 with amastigotes. Inhibition of Arg and SYK with imatinib and entospletinib,
429 respectively, significantly reduced ERK1/2 phosphorylation, to a similar degree to
430 the MAPK/ERK inhibitors SCH772984 and trametinib (**Fig. 4A, B**). As expected,
431 PMA, the positive control, significantly increased ERK1/2 phosphorylation (**Fig. 4A,**
432 **B**). The inhibitors and activators followed similar trends for promastigote-induced
433 ERK activity (**Supplemental Fig. 2B**). Thus, we could modulate *Leishmania*-induced
434 ERK activity by both inhibitors and activators *in vitro*.
435
436 To further characterize the role of SYK and Arg in *Leishmania*-induced ERK
437 phosphorylation, we next isolated BMDM from mice lacking Abl family kinases

438 (*Arg*$^{-/-}$*Abl*$^{flox/flox}$*LysM Cre*$^{+}$ [hereafter termed *Arg*$^{-/-}$*Abl*$^{-/-}$ when discussing isolated
439 BMDM]), SYK (*SYK*$^{flox/flox}$ *Cre*$^{+}$, abbreviated *SYK*$^{-/-}$ when referring to isolated BMDM)
440 or wild type (*WT*) littermates. We have previously shown that amastigote uptake is
441 dependent upon Arg but not Abl [15-16]. Our immunoblots showed *Arg*$^{-/-}$*Abl*$^{-/-}$ and
442 *SYK*$^{-/-}$ BMDM nearly completely lack Arg or SYK, respectively, while ERK1/2
443 expression was maintained (**Supplemental Fig. 2C**). Consistent with our chemical
444 inhibition experiments, SYK$^{-/-}$ and *Arg*$^{-/-}$*Abl*$^{-/-}$ BMDM limited amastigote-mediated
445 ERK1/2 phosphorylation, demonstrating that SYK and Arg/Abl are necessary for
446 stimulating ERK1/2 phosphorylation following engagement of the FcγR (**Fig. 4C, D**).
447 At low doses (250 nM), PMA rescued ERK1/2 activity in *Arg*$^{-/-}$*Abl*$^{-/-}$ and *SYK*$^{-/-}$
448 BMDM. This suggested 1) amastigotes operate through a distinct pathway to
449 activate ERK1/2 compared to PMA, which activates MAPK/ERK through PKC [26]
450 and 2) during FcγR-mediated amastigote infection, Arg and SYK family kinases are
451 upstream of MAPK/ERK and are necessary to activate the MAPK/ERK pathway.
452
453 To directly test whether Abl family kinases are critical for ERK1/2-mediated
454 amastigote uptake, we treated *WT* and *Arg*$^{-/-}$*Abl*$^{-/-}$ BMDM with DMSO or PMA prior
455 to infection with IgG-opsonized amastigotes. We found that *Arg*$^{-/-}$ *Abl*$^{-/-}$ BMDM
456 displayed defects in IgG-mediated amastigote uptake, while PMA treatment partially
457 rescued these defects (**Fig. 4E-G**), returning uptake to 66.4 ± 16.6% (mean ± SD)
458 compared to 29.3 ± 0.9% with DMSO. Similarly, SYK was necessary for efficient
459 amastigote uptake, and the decreased PI of *SYK*$^{-/-}$ BMDM was partially rescued by
460 PMA treatment (**Supplemental Fig. 2D, E)**. Taken together, these results, in

461 combination with prior data, are consistent with a signaling pathway in which Arg/Abl
462 and SYK act upstream of and activate the ERK1/2 pathway (which is at least partly
463 independent from PKC) to facilitate amastigote uptake [26].
464
465 **3.5 MAPK/ERK inhibition minimally impacts phagocytosis of opsonized beads**
466 *Arg*$^{-/-}$ BMDM have been shown to have impaired FcR-mediated phagocytosis
467 overall, as demonstrated using IgG-coated (opsonized) beads [17]. Thus, we
468 hypothesized that the Arg-SYK-ERK pathway may be necessary for the general
469 process of phagocytosis, in addition to amastigote uptake. To delineate the specific
470 contributions of MAPK/ERK to phagocytosis, we examined bead uptake compared
471 to amastigote uptake by RAW 264.7 cells. Surprisingly, phagocytosis of IgG-
472 opsonized beads by RAW 264.7 cells was minimally affected by trametinib (**Fig. 5A,**
473 **B**) or SCH772984 (**Supplemental Fig. 3),** both of which resulted in only a ~30%
474 reduction in uptake. Conversely, the uptake of IgG-coated amastigotes (**Fig. 1)** was
475 reduced by ~70% with trametinib treatment. However, when RAW 264.7 cells were
476 treated with imatinib, similar decreases in phagocytosis of IgG-opsonized beads
477 versus amastigotes were observed. These results suggest that Arg/Abl play a more
478 generalized role in phagocytosis, as we have demonstrated previously [17].
479 Collectively, our data suggest that ERK1/2 activation is important for *Leishmania*
480 uptake specifically but may play a minor role in standard phagocytic mechanisms.
481
482 We also tested whether MAPK/ERK activity was induced following addition of beads
483 compared to amastigotes. Beads induced ERK1/2 phosphorylation, but to levels that

484 were lower than in seen during amastigote uptake (**Fig. 5C, D**). This phosphorylation
485 occurred in a time-dependent fashion, such that activation reached maximal levels
486 between 5 and 10 m, and ERK1/2 phosphorylation was not detectable after 30 m
487 (**Fig. 5C, D**). Similarly, beads activated upstream kinases MEK1/2 (**Fig. 5E, F)** and
488 cRaf (**Fig. 5G, H**); however, their phosphorylation was not sustained. Thus, in
489 contrast to the sustained activation of MAPK/ERK that we saw during amastigote
490 uptake, beads had only a transient effect on ERK1/2 activation.
491
492 **3.6 Trametinib increases the intensity of actin labeled in phagocytic cups.**
493 Next, we explored the mechanisms by which trametinib affected *Leishmania*
494 amastigote internalization. We first characterized trametinib's effects on phagocytic
495 cup formation by performing an internalization assay with amastigotes as described
496 above, with the addition of fluorescent phalloidin to label phagocytic cups. We found
497 that phalloidin labeling of phagocytic cups was significantly brighter in trametinib-
498 treated Mϕs on average than DMSO-treated Mϕs, suggesting direct effects on
499 polymerization during the formation of actin-rich phagocytic cups (**Supplemental**
500 **Fig. 4A-C**). We next calculated the percentages of Mϕs infected by amastigotes and
501 the average numbers of amastigotes per infected Mϕ. We found that both were
502 affected by trametinib at approximately the values expected from the decrease in
503 phagocytic indexes (**Supplemental Fig. 4D-E**).
504
505 **3.7 Trametinib decreases lesion size and parasite burden in a murine model of**
506 **cutaneous leishmaniasis.** To test whether the MAPK/ERK pathway is necessary

507 for *Leishmania* pathogenesis *in vivo*, we employed a C57BL/6 mouse model of
508 cutaneous leishmaniasis using *L. amazonensis.* Footpad swelling (*i.e*., lesion size)
509 was measured in infected mice treated with 2 mg/kg of body weight/day of oral
510 trametinib or drug vehicle (control) starting 7 days (d) before inoculation and
511 continuing for the experimental duration of 14-16 weeks (w) [16, 17] (**Fig. 6A**).
512 Compared to controls, trametinib-treated mice developed smaller lesions (**Fig. 6B**),
513 which contained fewer parasites in lesions (**Fig. 6C**). The decreased number of
514 parasites found within lesions may help to explain these changes in lesion size.
515
516 Overall, in leishmaniasis, as a simplified paradigm, a Th1 response is thought to
517 be beneficial to the host, while a Th2 response is typically considered to be
518 deleterious. To determine whether the immunological effects of MEK1/2 inhibition
519 were associated with the healing seen in trametinib-treated mice, we isolated
520 draining lymph nodes from infected DMSO and trametinib-treated mice. We then
521 profiled cytokine and chemokine secretion after stimulation with high (1×10^6) or
522 low (1×10^5) doses of *L. amazonensis* lysates compared to unstimulated. A mild
523 shift in the overall ratio of Th1 to Th2 cytokines (Th1/Th2) towards a Th2
524 phenotype in trametinib-treated mice was seen (**Table 1**). Notably, lymph nodes
525 extracted from trametinib-treated mice released lower quantities of nearly all
526 cytokines in response to *L. amazonensis* than those isolated from diluent-treated
527 animals (**Table 2**). Trametinib-treated mice also demonstrated decreased
528 cytokine production in response to concanavalin A (Con A) stimulation. In
529 addition, we assessed chemokine secretion following MEK1/2 inhibition. The

530 production of several chemokines implicated in *Leishmania* pathogenesis,
531 including MIP-1α (CCL3) and MCP-1 (CCL2), were significantly decreased with
532 trametinib (**Table 2**), consistent with the decrease in cytokines/chemokines
533 overall.
534
535 We further tested whether MEK1/2 inhibition with trametinib reduces pathogenesis
536 after the development of symptoms by infecting mice as above. However, we started
537 diluent vs trametinib at 6 w after inoculation (*i.e.*, once lesions were clearly visible)
538 and continued therapy for the remaining experimental duration (**Fig. 6D**). Even with
539 this delayed treatment, trametinib-treated mice reproducibly had smaller lesions
540 (**Fig. 6E**). They also had significantly lower parasite burdens than those of controls
541 (**Fig. 6F**), which at least in part may explain these results. We also saw similar
542 immunological responses in mice treated with trametinib initiated partway through
543 the experiment as we did for the mice treated prior to *Leishmania* infection
544 (**Supplemental Table 1, Supplemental Table 2**) [53, 54]. Overall, our findings
545 demonstrate that trametinib administration limits the manifestations of leishmaniasis
546 in a mouse model, even if it is started after lesions have developed.

547 **4. DISCUSSION**

548 Here, we have shown that efficient *Leishmania* uptake by Mϕs and infection in mice
549 requires MAPK/ERK. While previous studies have shown that ERK1/2 activation
550 post-infection by *Leishmania* alters various host signaling pathways, leading to
551 increased intracellular survival and replication of these parasites [36, 55], our results
552 establish an earlier role for host ERK1/2 activity during the *Leishmania* life cycle, and
553 show that ERK1/2 is necessary for efficient *Leishmania* uptake into Mϕs.
554 Furthermore, our results delineate new activators of ERK signaling, and suggest that
555 MAPK/ERK affects actin polymerization. In combination with prior data, we propose
556 a model whereby, following engagement of the FcγR, host Arg/Abl and SYK
557 stimulate Raf, MEK, and ERK1/2 phosphorylation, leading to amastigote uptake
558 (**Fig. 6G**). Moreover, *in vivo* inhibition of MEK1/2 by trametinib in a mouse model of
559 cutaneous leishmaniasis significantly limits lesion development and parasite burden,
560 even when trametinib is started after these lesions have developed. Our results
561 highlight a critical role for MAPK/ERK signaling in *Leishmania* uptake and further
562 previously published studies of its role in the pathogenesis of leishmaniasis.
563

564 Our data indicate that Arg/Abl and SYK are required for amastigote-mediated
565 ERK1/2 phosphorylation following FcγR activation, which has not been
566 demonstrated previously. Our prior studies of host signaling required for *Leishmania*
567 uptake revealed that amastigotes bind directly to FcγR [15] and activate SFK-Arg
568 pathways [16] to induce uptake. We conclude from our combined results that an
569 FcγR-SFK-Arg-SYK signaling pathway functions upstream of and activates

570 MAPK/ERK family kinases, which in turn affects the intensity of polymerized actin in
571 phagocytic cups. We previously published similar effects on actin polymerization
572 using the SYK inhibitor entospletinib during *Leishmania* uptake [18]. Interestingly,
573 pharmacological inhibition of MEK1/2 and ERK1/2 in RAW 264.7 cells significantly
574 reduce, but does not completely abolish, *Leishmania* uptake. One explanation for
575 these results is that kinase inhibition via these compounds may be incomplete.
576 Another is that *Leishmania* uptake may be mediated via additional host signaling
577 pathways. Supporting the latter hypothesis, we find that low or sub-EC_{50} doses of
578 PMA, which activates ERK1/2 through an SFK-Arg-SYK-independent manner,
579 rescues trametinib inhibition of *Leishmania* amastigote uptake in RAW 264.7 cells,
580 as well as in *SYK*$^{-/-}$ and *Arg*$^{-/-}$*Abl*$^{-/-}$ BMDM. PMA is a known activator of PKC [26,
581 56-60]. However, we find that PKC activity is only slightly increased during
582 amastigote infection of WT/DMSO-treated Mϕs, suggesting that PKC may play only
583 a minor role during typical amastigote uptake. Ongoing work in the laboratory is
584 directed at uncovering additional novel uptake mechanisms for *Leishmania*. In
585 addition, although drug combinations typically are not used to treat leishmaniasis,
586 they are the standard of care for many other infections, such as HIV or tuberculosis.
587 Combination therapy with multiple kinase inhibitors to inhibit several uptake
588 modulators at once may provide additional benefit for the treatment of leishmaniasis
589 over single host cell kinase inhibitors alone.
590
591 Our data using MEK/ERK inhibitors indicate that there are differences in MAPK/ERK
592 signaling within Mϕs depending on whether *Leishmania* amastigotes or IgG-coated

593 beads are undergoing internalization. These results differ from most available
594 literature that concludes that *Leishmania* primarily hijacks ongoing phagocytic
595 pathways to facilitate its uptake. We instead suggest that there may be alternative,
596 perhaps partly redundant, pathways that may support the uptake of *Leishmania* over
597 the phagocytosis of beads, and vice versa. Our future experiments will continue to
598 compare and contrast the signaling pathways required for these different uptake
599 mechanisms between opsonized beads and *Leishmania* parasites.
600
601 Our experiments using a mouse model for *Leishmania* infection, in combination with
602 prior studies [33], show that MAPK/ERK are required for maximal *Leishmania*
603 pathogenesis during cutaneous leishmaniasis. One highly plausible explanation for
604 the decreased lesion size and parasite burden that we see in trametinib-treated mice
605 is our previously documented inhibition of *Leishmania* uptake, in combination with
606 previous studies suggesting MAPK/ERK signaling affects parasite survival in Mϕs
607 [26-33]. Consistent with this hypothesis, fewer parasites are found in lesions from
608 trametinib-treated mice than in control mice. Alternately, lesion size variations after
609 *L. amazonensis* infection might result from known trametinib limitation of host
610 inflammatory and immunological responses. Many pathogens hinder immune
611 responses by targeting host intracellular signaling pathways, including MAPK
612 pathways [59, 61]; and MAPKs have been shown to play roles in the immune
613 response to leishmaniasis [26-33]. The murine immune response to leishmaniasis is
614 complicated and varies depending on the species of *Leishmania* and the mouse
615 strain used. As a simplified paradigm, Th1 responses are generally protective, but

616 Th2 responses are harmful to the host [28, 31, 32]. We find that all cytokines
617 assessed following *Leishmania* antigen stimulation in lymph nodes isolated from
618 infected trametinib-treated mice are reduced from the levels seen in diluent-treated
619 mice, similar to our prior results using bosutinib [16]. One possible explanation is that
620 fewer cytokines are generated because the lesions contain fewer parasites. Another
621 is that trametinib could instead dampen pathways important for maintaining an active
622 inflammatory response to the ongoing host response to infection. Supporting this
623 second possibility, cytokines measured after Con A stimulation (an antigen-
624 independent mitogen used as an alternative T cell stimulus) are significantly reduced
625 by MEK1/2 inhibition. Overall, the moderate shift in the total ratio of Th1 to Th2
626 cytokines (Th1/Th2) toward a Th2 phenotype that we see theoretically should
627 exacerbate disease rather than alleviate it. We do note a surprisingly strong IL-10
628 response in the trametinib-treated mice, considering that ERK activation has been
629 shown to be required for IL-10 production by *Leishmania*-infected Mϕs [62].
630 However, others have found that trametinib treatment increases IL-10 production in
631 mouse tissues [63]. Reduced levels of proinflammatory chemokines like MIP-1
632 (CCL3) and MCP-1 (CCL2), on the other hand, may be responsible for reducing
633 lesion size by restricting the number of immune cells, especially phagocytic cells,
634 which reach the site of infection. Further work is needed to delineate the regulation
635 of immune responses to *Leishmania* infection and the resulting effects on lesion
636 worsening versus healing.
637

638 Finally, and of particular interest, we have demonstrated that there are reductions
639 in lesion size and parasite burden if trametinib is used in a *L. amazonensis*
640 mouse model of cutaneous leishmaniasis, even if it is started after foot swelling
641 has developed. Compared to our previous results, the data shown here strongly
642 suggest that trametinib is more effective for reducing lesion size than imatinib
643 [17] or bosutinib [16], which target signaling molecules in the same pathway.
644 Trametinib is used clinically to treat several cancers, making it feasible that this
645 drug could be repurposed to treat an infectious disease, and facilitating potential
646 clinical trials for its use against leishmaniasis. Our data imply that inhibiting a
647 signaling pathway downstream of SFK-Arg-SYK might improve results over
648 inhibiting kinases upstream in the pathway. Our results also give credence to our
649 overarching hypothesis that targeting host cell pathways, particularly ones that
650 are required for multiple aspects of the parasite life cycle and pathogenesis, may
651 permit treatment of an infectious disease such as leishmaniasis.
652

653 **5. CONCLUSIONS**

654 In summary, we have demonstrated that Arg-SYK signaling through MAPK/ERK
655 facilitates *Leishmania* uptake by Mϕ. Furthermore, ERK activity helps govern the
656 subsequent pathogenesis and disease progression of leishmaniasis in the mouse
657 model. Due to the relative specificity of newer-generation MAPK/ERK small
658 molecule inhibitors like trametinib, it is possible to selectively target MEK1/2 and
659 ERK1/2 for potential therapeutic intervention. Our findings demonstrate the
660 significance of MAPK/ERK signaling during *Leishmania* entry into phagocytic cells.

661 Our future studies will investigate the use of host-cell-active drugs, potentially in
662 conjunction with other kinase inhibitors or existing antiparasitics, to improve efficacy,
663 decrease toxicity, and limit the likelihood of developing resistance. Although
664 trametinib is not completely without side effects, this combination strategy could be
665 used to mitigate any risk of toxicity arising due to targeting essential signaling
666 pathways. Furthermore, our results support the novel possibility that medications
667 that target conserved host cell processes rather than infectious pathogens might be
668 employed to treat a wide spectrum of intracellular pathogens.
669

670 **6. ACKNOWLEDGEMENTS**

671 We thank Drs. Neal M. Alto, Melanie H. Cobb, Margaret A. Phillips, James J.
672 Collins, and Michael L. Reese (all at UT Southwestern) for helpful discussions
673 and feedback. Members of the UT Southwestern Departments of Pediatrics,
674 Biochemistry, Microbiology, and Pharmacology provided valuable feedback and
675 permitted common equipment use. Francis Khuong and Catherine Trice provided
676 expert technical assistance and helped to edit this manuscript. Dr. Diane
677 McMahon-Pratt (Yale University) generously donated antileishmanial antibodies.
678 Dr. Anthony J. Koleske (Yale University) provided the *Arg*$^{-/-}$*Abl*$^{flox/flox}$ mice. The
679 UT Southwestern Microarray Core assisted with cytokine/chemokine profiling.
680

681 **Funding:** This work was supported by a Children's Clinical Research Advisory
682 Committee (CCRAC) Junior Investigator Award, a CCRAC Early Investigator
683 Award, the National Institutes of Health (K08 AI103036 and R01 AI146349),
684 Welch Foundation Grant I-2048, and the UT Southwestern Department of
685 Pediatrics (to D.M.W.). U.B. was supported by a National Institutes of Health
686 Supplement to Promote Diversity in Health-Related Research (R01 AI146349-
687 S1) and Medical Scientist Training (MD/PhD) Grant NIH T32GM008014. K.F.
688 was supported by a UT Southwestern-Amgen Summer Research Fellowship.
689

690 **Competing interests:** The authors have no competing financial interests.
691

Data and materials availability: All data are available within the main text of the manuscript or the supplemental materials. Any materials generated for this manuscript are freely available upon request.

696 **7. REFERENCES AND NOTES**:

697 1. Gossage SM, Rogers ME, Bates PA. Two separate growth phases during the
698 development of Leishmania in sand flies: implications for understanding the life cycle. Int
699 J Parasitol. 2003;33(10):1027-34. doi: 10.1016/s0020-7519(03)00142-5. PubMed PMID:
700 13129524; PubMed Central PMCID: PMCPMC2839921.

701 2. Markle WH, Makhoul K. Cutaneous leishmaniasis: recognition and treatment. Am
702 Fam Physician. 2004;69(6):1455-60. PubMed PMID: 15053410.

703 3. McCall LI, Zhang WW, Matlashewski G. Determinants for the development of
704 visceral leishmaniasis disease. PLoS Pathog. 2013;9(1):e1003053. doi:
705 10.1371/journal.ppat.1003053. PubMed PMID: 23300451; PubMed Central PMCID:
706 PMCPMC3536654.

707 4. Georgiadou SP, Makaritsis KP, Dalekos GN. Leishmaniasis revisited: Current
708 aspects on epidemiology, diagnosis and treatment. J Transl Int Med. 2015;3(2):43-50.
709 doi: 10.1515/jtim-2015-0002. PubMed PMID: 27847886; PubMed Central PMCID:
710 PMCPMC4936444.

711 5. Steverding D. The history of leishmaniasis. Parasit Vectors. 2017;10(1):82. Epub
712 2017/02/17. doi: 10.1186/s13071-017-2028-5. PubMed PMID: 28202044; PubMed
713 Central PMCID: PMCPMC5312593.

714 6. Gonzalez C, Wang O, Strutz SE, Gonzalez-Salazar C, Sanchez-Cordero V, Sarkar
715 S. Climate change and risk of leishmaniasis in North America: predictions from ecological
716 niche models of vector and reservoir species. PLoS Negl Trop Dis. 2010;4(1):e585. Epub
717 2010/01/26. doi: 10.1371/journal.pntd.0000585. PubMed PMID: 20098495; PubMed
718 Central PMCID: PMCPMC2799657.

719 7. McIlwee BE, Weis SE, Hosler GA. Incidence of endemic human cutaneous
720 leishmaniasis in the United States. JAMA Dermatol. 2018;154(9):1032-9. doi:
721 10.1001/jamadermatol.2018.2133. PubMed PMID: 30046836; PubMed Central PMCID:
722 PMCPMC6143046.
723 8. Croft SL, Sundar S, Fairlamb AH. Drug resistance in leishmaniasis. Clin Microbiol
724 Rev. 2006;19(1):111-26. Epub 2006/01/19. doi: 10.1128/CMR.19.1.111-126.2006.
725 PubMed PMID: 16418526; PubMed Central PMCID: PMCPMC1360270.
726 9. Elmahallawy EK, Agil A. Treatment of leishmaniasis: a review and assessment of
727 recent research. Curr Pharm Des. 2015;21(17):2259-75. Epub 2014/12/30. doi:
728 10.2174/1381612821666141231163053. PubMed PMID: 25543123.
729 10. Mann S, Frasca K, Scherrer S, Henao-Martinez AF, Newman S, Ramanan P, et
730 al. A review of leishmaniasis: current knowledge and future directions. Curr Trop Med
731 Rep. 2021;8(2):121-32. Epub 2021/03/23. doi: 10.1007/s40475-021-00232-7. PubMed
732 PMID: 33747716; PubMed Central PMCID: PMCPMC7966913.
733 11. Ponte-Sucre A, Gamarro F, Dujardin JC, Barrett MP, Lopez-Velez R, Garcia-
734 Hernandez R, et al. Drug resistance and treatment failure in leishmaniasis: A 21st century
735 challenge. PLoS Negl Trop Dis. 2017;11(12):e0006052. Epub 2017/12/15. doi:
736 10.1371/journal.pntd.0006052. PubMed PMID: 29240765; PubMed Central PMCID:
737 PMCPMC5730103.
738 12. Handman E, Bullen DV. Interaction of *Leishmania* with the host macrophage.
739 Trends Parasitol. 2002;18(8):332-4. doi: 10.1016/s1471-4922(02)02352-8. PubMed
740 PMID: 12377273.

741 13. Alexander J, Russell DG. The interaction of Leishmania species with
742 macrophages. Adv Parasitol. 1992;31:175-254. Epub 1992/01/01. doi: 10.1016/s0065-
743 308x(08)60022-6. PubMed PMID: 1496927.
744 14. Kima PE. The amastigote forms of Leishmania are experts at exploiting host cell
745 processes to establish infection and persist. Int J Parasitol. 2007;37(10):1087-96. doi:
746 10.1016/j.ijpara.2007.04.007. PubMed PMID: 17543969; PubMed Central PMCID:
747 PMCPMC2043126.
748 15. Ueno N, Wilson ME. Receptor-mediated phagocytosis of Leishmania: implications
749 for intracellular survival. Trends Parasitol. 2012;28(8):335-44. doi:
750 10.1016/j.pt.2012.05.002. PubMed PMID: 22726697; PubMed Central PMCID:
751 PMCPMC3399048.
752 16. Wetzel DM, Rhodes EL, Li S, McMahon-Pratt D, Koleske AJ. The Src kinases Hck,
753 Fgr and Lyn activate Arg to facilitate IgG-mediated phagocytosis and Leishmania
754 infection. J Cell Sci. 2016;129(16):3130-43. Epub 2016/07/01. doi: 10.1242/jcs.185595.
755 PubMed PMID: 27358479; PubMed Central PMCID: PMCPMC5004897.
756 17. Wetzel DM, McMahon-Pratt D, Koleske AJ. The Abl and Arg kinases mediate
757 distinct modes of phagocytosis and are required for maximal *Leishmania* infection. Mol
758 Cell Biol. 2012;32(15):3176-86. Epub 2012/06/06. doi: 10.1128/MCB.00086-12. PubMed
759 PMID: 22665498; PubMed Central PMCID: PMCPMC3434515.
760 18. Ullah I, Barrie U, Kernen RM, Mamula ET, Khuong FTH, Booshehri LM, et al. Src-
761 and Abl-family kinases activate spleen tyrosine kinase to maximize phagocytosis and
762 *Leishmania* infection. J Cell Sci. 2023;136(14). Epub 2023/06/26. doi:

763 10.1242/jcs.260809. PubMed PMID: 37357611; PubMed Central PMCID:
764 PMCPMC10399977.
765 19. Greuber EK, Pendergast AM. Abl family kinases regulate FcgammaR-mediated
766 phagocytosis in murine macrophages. J Immunol. 2012;189(11):5382-92. Epub
767 2012/10/27. doi: 10.4049/jimmunol.1200974. PubMed PMID: 23100514; PubMed Central
768 PMCID: PMCPMC3504141.
769 20. Ortiz MA, Mikhailova T, Li X, Porter BA, Bah A, Kotula L. Src family kinases,
770 adaptor proteins and the actin cytoskeleton in epithelial-to-mesenchymal transition. Cell
771 Commun Signal. 2021;19(1):67. Epub 2021/07/02. doi: 10.1186/s12964-021-00750-x.
772 PubMed PMID: 34193161; PubMed Central PMCID: PMCPMC8247114.
773 21. Cortez D, Reuther G, Pendergast AM. The Bcr-Abl tyrosine kinase activates
774 mitogenic signaling pathways and stimulates G1-to-S phase transition in hematopoietic
775 cells. Oncogene. 1997;15(19):2333-42. Epub 1997/12/11. doi: 10.1038/sj.onc.1201400.
776 PubMed PMID: 9393877.
777 22. Jin A, Kurosu T, Tsuji K, Mizuchi D, Arai A, Fujita H, et al. BCR/ABL and IL-3
778 activate Rap1 to stimulate the B-Raf/MEK/Erk and Akt signaling pathways and to regulate
779 proliferation, apoptosis, and adhesion. Oncogene. 2006;25(31):4332-40. Epub
780 2006/03/07. doi: 10.1038/sj.onc.1209459. PubMed PMID: 16518411.
781 23. Yang S, Liu G. Targeting the Ras/Raf/MEK/ERK pathway in hepatocellular
782 carcinoma. Oncol Lett. 2017;13(3):1041-7. Epub 2017/04/30. doi: 10.3892/ol.2017.5557.
783 PubMed PMID: 28454211; PubMed Central PMCID: PMCPMC5403244.
784 24. Guo YJ, Pan WW, Liu SB, Shen ZF, Xu Y, Hu LL. ERK/MAPK signalling pathway
785 and tumorigenesis. Exp Ther Med. 2020;19(3):1997-2007. Epub 2020/02/28. doi:

786 10.3892/etm.2020.8454. PubMed PMID: 32104259; PubMed Central PMCID:
787 PMCPMC7027163.
788 25. Eblen ST. Extracellular-Regulated Kinases: signaling From Ras to ERK substrates
789 to control biological outcomes. Adv Cancer Res. 2018;138:99-142. Epub 2018/03/20. doi:
790 10.1016/bs.acr.2018.02.004. PubMed PMID: 29551131; PubMed Central PMCID:
791 PMCPMC6007982.
792 26. Verin AD, Liu F, Bogatcheva N, Borbiev T, Hershenson MB, Wang P, et al. Role
793 of ras-dependent ERK activation in phorbol ester-induced endothelial cell barrier
794 dysfunction. Am J Physiol Lung Cell Mol Physiol. 2000;279(2):L360-70. Epub 2000/08/05.
795 doi: 10.1152/ajplung.2000.279.2.L360. PubMed PMID: 10926560.
796 27. Wu X, Dayanand KK, Thylur RP, Norbury CC, Gowda DC. Small molecule-based
797 inhibition of MEK1/2 proteins dampens inflammatory responses to malaria, reduces
798 parasite load, and mitigates pathogenic outcomes. J Biol Chem. 2017;292(33):13615-34.
799 Epub 2017/07/07. doi: 10.1074/jbc.M116.770313. PubMed PMID: 28679535; PubMed
800 Central PMCID: PMCPMC5566520.
801 28. Martinez PA, Petersen CA. Chronic infection by *Leishmania amazonensis*
802 mediated through MAPK ERK mechanisms. Immunol Res. 2014;59(1-3):153-65. Epub
803 2014/05/20. doi: 10.1007/s12026-014-8535-y. PubMed PMID: 24838145; PubMed
804 Central PMCID: PMCPMC4686340.
805 29. Shadab M, Ali N. Evasion of host defence by *Leishmania donovani*: subversion of
806 signaling pathways. Mol Biol Int. 2011;2011:343961. Epub 2011/11/18. doi:
807 10.4061/2011/343961. PubMed PMID: 22091401; PubMed Central PMCID:
808 PMCPMC3199940.

809 30. Olivier M, Gregory DJ, Forget G. Subversion mechanisms by which Leishmania
810 parasites can escape the host immune response: a signaling point of view. Clin Microbiol
811 Rev. 2005;18(2):293-305. Epub 2005/04/16. doi: 10.1128/CMR.18.2.293-305.2005.
812 PubMed PMID: 15831826; PubMed Central PMCID: PMCPMC1082797.
813 31. Ghalib HW, Whittle JA, Kubin M, Hashim FA, el-Hassan AM, Grabstein KH, et al.
814 IL-12 enhances Th1-type responses in human *Leishmania donovani* infections. J
815 Immunol. 1995;154(9):4623-9. Epub 1995/05/01. PubMed PMID: 7722314.
816 32. Bhardwaj S, Srivastava N, Sudan R, Saha B. Leishmania interferes with host cell
817 signaling to devise a survival strategy. J Biomed Biotechnol. 2010;2010:109189. Epub
818 2010/04/17. doi: 10.1155/2010/109189. PubMed PMID: 20396387; PubMed Central
819 PMCID: PMCPMC2852600.
820 33. Yang Z, Mosser DM, Zhang X. Activation of the MAPK, ERK, following *Leishmania*
821 *amazonensis* infection of macrophages. J Immunol. 2007;178(2):1077-85. doi:
822 10.4049/jimmunol.178.2.1077. PubMed PMID: 17202371; PubMed Central PMCID:
823 PMCPMC2643020.
824 34. Mukbel RM, Patten C, Jr., Gibson K, Ghosh M, Petersen C, Jones DE.
825 Macrophage killing of *Leishmania amazonensis* amastigotes requires both nitric oxide
826 and superoxide. Am J Trop Med Hyg. 2007;76(4):669-75. Epub 2007/04/12. PubMed
827 PMID: 17426168.
828 35. Calegari-Silva TC, Pereira RM, De-Melo LD, Saraiva EM, Soares DC, Bellio M, et
829 al. NF-kappaB-mediated repression of iNOS expression in *Leishmania amazonensis*
830 macrophage infection. Immunol Lett. 2009;127(1):19-26. Epub 2009/08/29. doi:
831 10.1016/j.imlet.2009.08.009. PubMed PMID: 19712696.

832 36. Boggiatto PM, Martinez PA, Pullikuth A, Jones DE, Bellaire B, Catling A, et al.
833 Targeted extracellular signal-regulated kinase activation mediated by *Leishmania*
834 *amazonensis* requires MP1 scaffold. Microbes Infect. 2014;16(4):328-36. doi:
835 10.1016/j.micinf.2013.12.006. PubMed PMID: 24463270; PubMed Central PMCID:
836 PMCPMC4023638.
837 37. Uphoff CC, Drexler HG. Eradication of mycoplasma contaminations. Methods Mol
838 Biol. 2013;946:15-26. Epub 2012/11/28. doi: 10.1007/978-1-62703-128-8_2. PubMed
839 PMID: 23179823.
840 38. Ullah I, Gahalawat S, Booshehri LM, Niederstrasser H, Majumdar S, Leija C, et al.
841 An antiparasitic compound from the Medicines for Malaria Venture Pathogen Box
842 promotes *Leishmania* tubulin polymerization. ACS Infect Dis. 2020;6(8):2057-72. Epub
843 2020/07/21. doi: 10.1021/acsinfecdis.0c00122. PubMed PMID: 32686409.
844 39. Wetzel DM, Hakansson S, Hu K, Roos D, Sibley LD. Actin filament polymerization
845 regulates gliding motility by apicomplexan parasites. Mol Biol Cell. 2003;14(2):396-406.
846 doi: 10.1091/mbc.E02-08-0458. PubMed PMID: 12589042; PubMed Central PMCID:
847 PMC149980.
848 40. Pan AA, McMahon-Pratt D. Monoclonal antibodies specific for the amastigote
849 stage of *Leishmania pifanoi*. I. Characterization of antigens associated with stage- and
850 species-specific determinants. J Immunol. 1988;140(7):2406-14. PubMed PMID:
851 2450920.
852 41. Champsi J, McMahon-Pratt D. Membrane glycoprotein M-2 protects against
853 *Leishmania amazonensis* infection. Infect Immun. 1988;56(12):3272-9. PubMed PMID:
854 3182080; PubMed Central PMCID: PMCPMC259734.

855 42. Soong L, Chang CH, Sun J, Longley BJ, Jr., Ruddle NH, Flavell RA, et al. Role of
856 CD4+ T cells in pathogenesis associated with *Leishmania amazonensis* infection. J
857 Immunol. 1997;158(11):5374-83. PubMed PMID: 9164958.
858 43. Soong L, Henard CA, Melby PC. Immunopathogenesis of non-healing American
859 cutaneous leishmaniasis and progressive visceral leishmaniasis. Semin Immunopathol.
860 2012;34(6):735-51. Epub 2012/10/12. doi: 10.1007/s00281-012-0350-8. PubMed PMID:
861 23053396; PubMed Central PMCID: PMCPMC4111229.
862 44. Navas A, Vargas DA, Freudzon M, McMahon-Pratt D, Saravia NG, Gomez MA.
863 Chronicity of dermal leishmaniasis caused by *Leishmania panamensis* is associated with
864 parasite-mediated induction of chemokine gene expression. Infect Immun.
865 2014;82(7):2872-80. doi: 10.1128/IAI.01133-13. PubMed PMID: 24752514; PubMed
866 Central PMCID: PMCPMC4097649.
867 45. Gonzalez-Fajardo L, Fernandez OL, McMahon-Pratt D, Saravia NG. *Ex vivo* host
868 and parasite response to antileishmanial drugs and immunomodulators. PLoS Negl Trop
869 Dis. 2015;9(5):e0003820. Epub 2015/05/30. doi: 10.1371/journal.pntd.0003820. PubMed
870 PMID: 26024228; PubMed Central PMCID: PMC4449175.
871 46. Falchook GS, Lewis KD, Infante JR, Gordon MS, Vogelzang NJ, DeMarini DJ, et
872 al. Activity of the oral MEK inhibitor trametinib in patients with advanced melanoma: a
873 phase 1 dose-escalation trial. Lancet Oncol. 2012;13(8):782-9. Epub 2012/07/19. doi:
874 10.1016/S1470-2045(12)70269-3. PubMed PMID: 22805292; PubMed Central PMCID:
875 PMCPMC4109286.

876 47. Cheng Y, Tian H. Current development status of MEK inhibitors. Molecules.
877 2017;22(10). Epub 2017/09/29. doi: 10.3390/molecules22101551. PubMed PMID:
878 28954413; PubMed Central PMCID: PMCPMC6151813.
879 48. Wong DJ, Robert L, Atefi MS, Lassen A, Avarappatt G, Cerniglia M, et al. Antitumor
880 activity of the ERK inhibitor SCH772984 [corrected] against BRAF mutant, NRAS mutant
881 and wild-type melanoma. Mol Cancer. 2014;13:194. Epub 2014/08/22. doi:
882 10.1186/1476-4598-13-194. PubMed PMID: 25142146; PubMed Central PMCID:
883 PMCPMC4155088.
884 49. Ciuffreda L, Del Bufalo D, Desideri M, Di Sanza C, Stoppacciaro A, Ricciardi MR,
885 et al. Growth-inhibitory and antiangiogenic activity of the MEK inhibitor PD0325901 in
886 malignant melanoma with or without BRAF mutations. Neoplasia. 2009;11(8):720-31.
887 Epub 2009/08/04. doi: 10.1593/neo.09398. PubMed PMID: 19649202; PubMed Central
888 PMCID: PMCPMC2713590.
889 50. Sun Y, Liu WZ, Liu T, Feng X, Yang N, Zhou HF. Signaling pathway of MAPK/ERK
890 in cell proliferation, differentiation, migration, senescence and apoptosis. J Recept Signal
891 Transduct Res. 2015;35(6):600-4. Epub 2015/06/23. doi:
892 10.3109/10799893.2015.1030412. PubMed PMID: 26096166.
893 51. Crowley MT, Costello PS, Fitzer-Attas CJ, Turner M, Meng F, Lowell C, et al. A
894 critical role for Syk in signal transduction and phagocytosis mediated by Fcgamma
895 receptors on macrophages. J Exp Med. 1997;186(7):1027-39. Epub 1997/10/07. doi:
896 10.1084/jem.186.7.1027. PubMed PMID: 9314552; PubMed Central PMCID:
897 PMCPMC2199061.

898 52. Kiefer F, Brumell J, Al-Alawi N, Latour S, Cheng A, Veillette A, et al. The Syk
899 protein tyrosine kinase is essential for Fcgamma receptor signaling in macrophages and
900 neutrophils. Mol Cell Biol. 1998;18(7):4209-20. Epub 1998/06/25. doi:
901 10.1128/MCB.18.7.4209. PubMed PMID: 9632805; PubMed Central PMCID:
902 PMCPMC109005.
903 53. Liu L, Mayes PA, Eastman S, Shi H, Yadavilli S, Zhang T, et al. The BRAF and
904 MEK inhibitors dabrafenib and trametinib: effects on immune function and in combination
905 with immunomodulatory antibodies Targeting PD-1, PD-L1, and CTLA-4. Clin Cancer
906 Res. 2015;21(7):1639-51. Epub 2015/01/16. doi: 10.1158/1078-0432.CCR-14-2339.
907 PubMed PMID: 25589619.
908 54. Shi-Lin D, Yuan X, Zhan S, Luo-Jia T, Chao-Yang T. Trametinib, a novel MEK
909 kinase inhibitor, suppresses lipopolysaccharide-induced tumor necrosis factor (TNF)-
910 alpha production and endotoxin shock. Biochem Biophys Res Commun.
911 2015;458(3):667-73. Epub 2015/02/17. doi: 10.1016/j.bbrc.2015.01.160. PubMed PMID:
912 25684183.
913 55. Boggiatto PM, Jie F, Ghosh M, Gibson-Corley KN, Ramer-Tait AE, Jones DE, et
914 al. Altered dendritic cell phenotype in response to *Leishmania amazonensis* amastigote
915 infection is mediated by MAP kinase, ERK. Am J Pathol. 2009;174(5):1818-26. doi:
916 10.2353/ajpath.2009.080905. PubMed PMID: 19349356; PubMed Central PMCID:
917 PMCPMC2671270.
918 56. Cheeseman KL, Ueyama T, Michaud TM, Kashiwagi K, Wang D, Flax LA, et al.
919 Targeting of protein kinase C-epsilon during Fcgamma receptor-dependent phagocytosis
920 requires the epsilonC1B domain and phospholipase C-gamma1. Mol Biol Cell.

921 2006;17(2):799-813. Epub 2005/12/02. doi: 10.1091/mbc.e04-12-1100. PubMed PMID:
922 16319178; PubMed Central PMCID: PMCPMC1356590.
923 57. Larsen EC, Ueyama T, Brannock PM, Shirai Y, Saito N, Larsson C, et al. A role
924 for PKC-epsilon in Fc gammaR-mediated phagocytosis by RAW 264.7 cells. J Cell Biol.
925 2002;159(6):939-44. Epub 2002/12/25. doi: 10.1083/jcb.200205140. PubMed PMID:
926 12499353; PubMed Central PMCID: PMCPMC2173999.
927 58. Panetti TS, Wilcox SA, Horzempa C, McKeown-Longo PJ. Alpha v beta 5 integrin
928 receptor-mediated endocytosis of vitronectin is protein kinase C-dependent. J Biol Chem.
929 1995;270(31):18593-7. Epub 1995/08/04. doi: 10.1074/jbc.270.31.18593. PubMed
930 PMID: 7543105.
931 59. Roy N, Chakraborty S, Paul Chowdhury B, Banerjee S, Halder K, Majumder S, et
932 al. Regulation of PKC mediated signaling by calcium during visceral leishmaniasis. PLoS
933 One. 2014;9(10):e110843. Epub 2014/10/21. doi: 10.1371/journal.pone.0110843.
934 PubMed PMID: 25329062; PubMed Central PMCID: PMCPMC4201563.
935 60. Zheleznyak A, Brown EJ. Immunoglobulin-mediated phagocytosis by human
936 monocytes requires protein kinase C activation. Evidence for protein kinase C
937 translocation to phagosomes. J Biol Chem. 1992;267(17):12042-8. Epub 1992/06/15.
938 PubMed PMID: 1376316.
939 61. Arthur JS, Ley SC. Mitogen-activated protein kinases in innate immunity. Nat Rev
940 Immunol. 2013;13(9):679-92. Epub 2013/08/21. doi: 10.1038/nri3495. PubMed PMID:
941 23954936.
942 62. Buxbaum LU, Scott P. Interleukin 10- and Fcgamma receptor-deficient mice
943 resolve *Leishmania mexicana* lesions. Infect Immun. 2005;73(4):2101-8. Epub

944 2005/03/24. doi: 10.1128/IAI.73.4.2101-2108.2005. PubMed PMID: 15784551; PubMed
945 Central PMCID: PMCPMC1087424.
946 63. Tada S, Anazawa T, Shindo T, Yamane K, Inoguchi K, Fujimoto N, et al. The MEK
947 inhibitor trametinib suppresses Major Histocompatibility Antigen-mismatched rejection
948 following pancreatic islet transplantation. Transplant Direct. 2020;6(9):e591. Epub
949 2020/08/28. doi: 10.1097/TXD.0000000000001045. PubMed PMID: 32851124; PubMed
950 Central PMCID: PMCPMC7423917.
951

952 **List of figures:**

953 **Figure 1.** The MAPK/ERK pathway is required for optimal amastigote uptake.

954 **Figure 2**. MAPK/ERK are activated during *Leishmania* uptake by Mϕ.

955 **Figure 3.** PMA activates ERK1/2 to modulate amastigote uptake.

956 **Figure 4.** SYK and Arg/Abl stimulate ERK1/2 phosphorylation during amastigote
957 uptake.

958 **Figure 5.** ERK 1/2's role in *Leishmania* uptake is greater than for phagocytosis of
959 beads.

960 **Figure 6.** MAPK/ERK permit efficient infection in a mouse model of cutaneous
961 leishmaniasis.

962 **Table 1.** Ongoing trametinib treatment during *L. amazonensis* infection has
963 limited effects on Th1 vs Th2 responses.

964 **Table 2.** Cytokine and chemokine profiles in diluent versus trametinib-treated,
965 *Leishmania*-infected mice.

966

967 **List of supplementary materials:**

968 **Supplemental Figure 1.** MAPK/ERK inhibitors decrease uptake and survival of
969 *L. amazonensis* promastigotes and amastigotes.

970 **Supplemental Figure 2.** Inhibiting kinases upstream of ERK during *L.*
971 *amazonensis* uptake decreases ERK phosphorylation.

972 **Supplemental Figure 3.** Inhibiting ERK1/2 has minimal effects on the uptake of
973 opsonized beads.

974 **Supplemental Figure 4.** Actin-based phagocytic cups are brighter in trametinib-
975 treated Mϕs taking up *Leishmania* amastigotes compared to DMSO-treated Mϕs.

976 **Supplemental Table 1.** Trametinib initiated during *L. amazonensis* infection has
977 limited effects on Th1 vs Th2 responses.

978 **Supplemental Table 2.** Cytokine and chemokine profiles from *Leishmania*-
979 infected mice treated once lesions are visible.

980 **Supplemental Table 3.** List of antibodies.

981 **FIGURES AND LEGENDS**

982 **Figure 1**

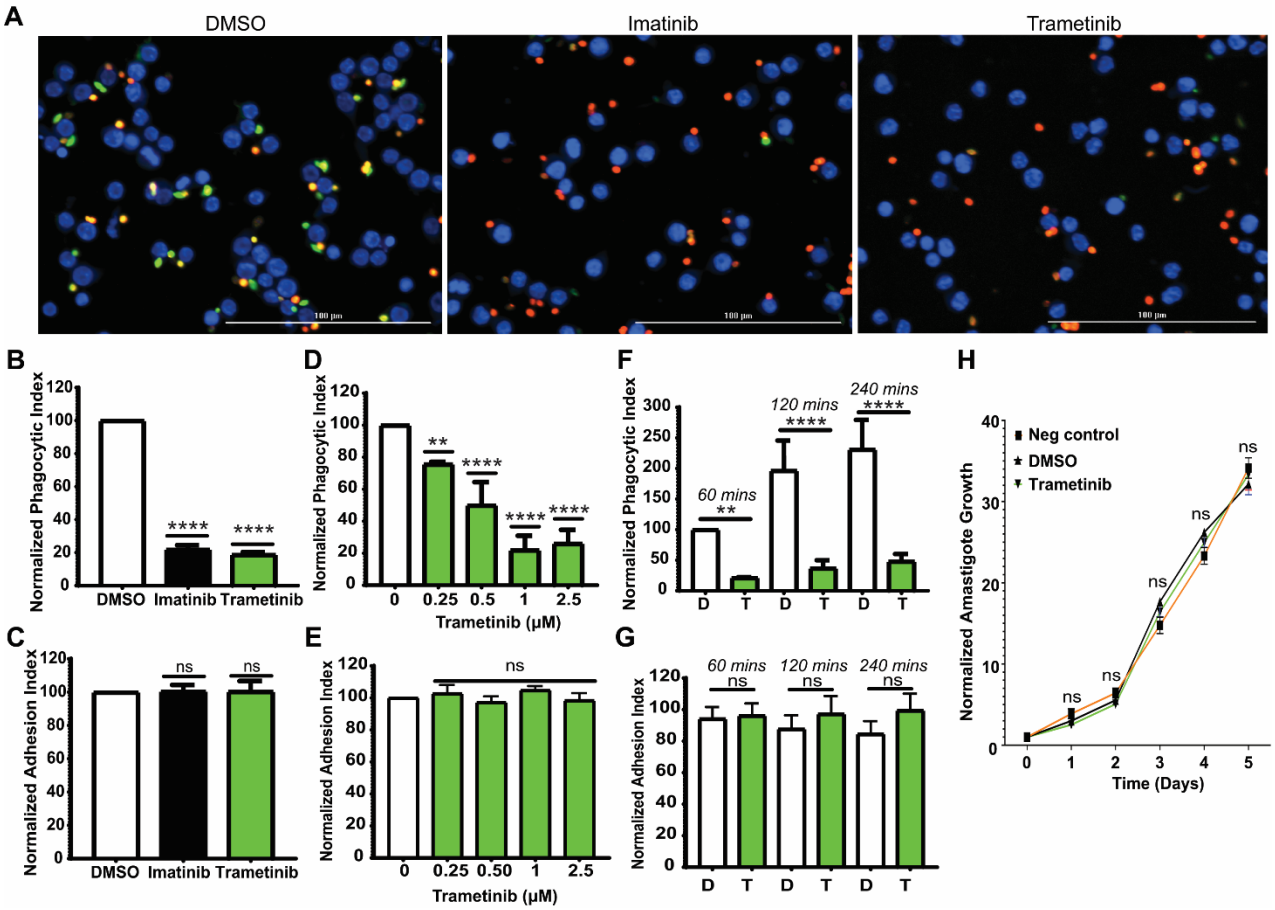

983

984 **Figure 1. The MAPK/ERK pathway is required for optimal amastigote**

985 **uptake. (A)** Trametinib decreases IgG-opsonized amastigote uptake. RAW 264.7

986 cells were treated with 3.3 μM imatinib, 1 μM trametinib or DMSO for 2 h, and 10

987 IgG-opsonized amastigotes were incubated per RAW 264.7 cell for 2 h at 37°C.

988 An immunofluorescence assay distinguished between intracellular (green) and

989 extracellular (red + green) amastigotes. Nuclei are labeled with Hoescht 33342

990 (blue). Scale bar, 100 μm. **(B)** Graph showing the mean phagocytic index (PI) ±

991 standard deviation (SD) for RAW 264.7 cells normalized to DMSO for each

992 experiment (100%), quantified from n = 6 biological experiments. Comparisons

993 between imatinib and trametinib by ANOVA were nonsignificant. **(C)** Imatinib and
994 trametinib do not affect the total (external + internal) number of amastigotes per
995 100 RAW cells (termed an adhesion index). Shown are percentages of total
996 amastigotes per 100 imatinib-treated and trametinib-treated RAW 264.7 cells
997 relative to DMSO-treated cells for the experiment shown in B. **(D)** Titration of
998 trametinib demonstrates that the reduction of amastigote internalization is
999 maximal at ~100x the purified MEK1/2 IC_{50}. RAW 264.7 cells were treated with
1000 increasing doses of trametinib (0.25, 0.5, 1, or 2.5 μM) or DMSO. Bar graph
1001 shows the mean PI ± SD for trametinib-treated samples relative to DMSO-treated
1002 samples for each experiment (100%) for 4 biological experiments. **(E)** The
1003 adhesion index for amastigotes from experiment in D is not affected by
1004 increasing doses of trametinib. Experiment performed as in C. **(F)** The relative
1005 decrease in PI for trametinib-treated samples persists even after prolonged
1006 incubation. RAW 264.7 cells were treated with DMSO (D) or 1 μM trametinib (T)
1007 prior to addition of IgG-opsonized amastigotes for 1 h, 2 h, or 4 h, as indicated.
1008 Shown is the mean PI ± SD for each time point for the trametinib-treated
1009 condition, relative to the DMSO-treated condition, calculated from 4 biological
1010 experiments. **(G)** Treating samples with trametinib for prolonged periods does not
1011 affect the adhesion index for amastigotes. Shown are the total number of
1012 amastigotes (internal + external) per 100 RAW 264.7 cells for the experiments
1013 performed in F. For all experiments, ** $P < 0.01$, **** $P < 0.0001$, ns =
1014 nonsignificant compared to the relevant DMSO-treated category by ANOVA. **(H)**
1015 Trametinib is not toxic to amastigotes. Shown is one representative experiment

1016 of five experiments with two technical replicates following the number of
1017 amastigotes growing in untreated, DMSO-treated, or trametinib-treated media
1018 over 5 days relative to on day 0. ns, $P > 0.05$ compared to DMSO category by
1019 ANOVA.
1020

1021 **Figure 2**

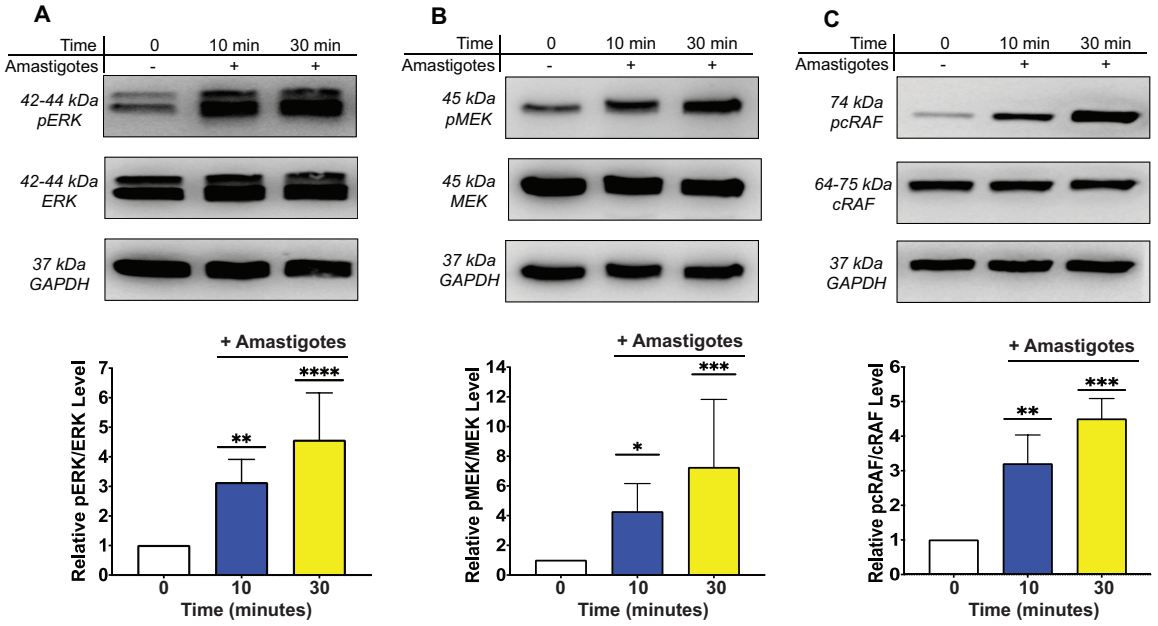

1022

1023 **Figure 2**. **MAPK/ERK are activated during *Leishmania* uptake by Mϕ.**

1024 Amastigotes were added to ≥ 70% confluent RAW 264.7 cells. Equal amounts of

1025 protein from whole lysates were employed for each category. **Top:**

1026 Representative blots displaying relative activation of MAPK/ERK. Phosphorylated

1027 **(A)** ERK1/2, **(B)** MEK1/2, **(C)** cRaf (Raf-1) and the corresponding total proteins

1028 were detected by Western Blot. An unrelated protein, GAPDH, is shown as an

1029 additional loading control. **Bottom:** Quantification of phosphorylated MAPK/ERK

1030 levels. Graphs shown in **(A)** for ERK1/2, **(B)** for MEK1/2, and **(C)** for cRaf

1031 represent mean ± SD of relative phosphorylated kinase levels, normalized to total

1032 kinase levels, for at least 3 biological replicates per condition. * $P < 0.05$, ** $P <$

1033 0.01, *** $P < 0.001$, **** $P < 0.0001$ by ANOVA compared to the 0 m time point

1034 for each set of kinases.

1035

1036 **Figure 3**

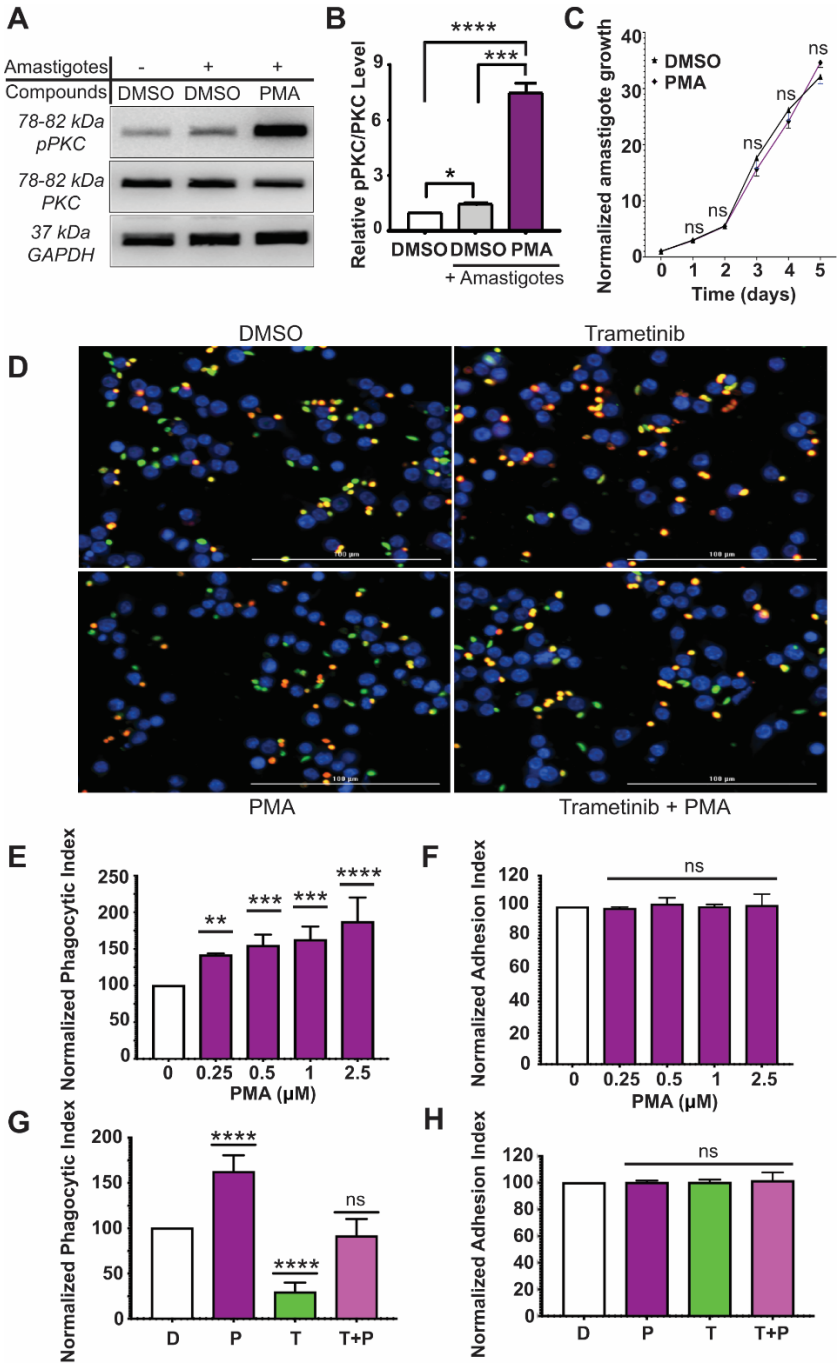

1037

1038 **Figure 3. PMA activates ERK1/2 to modulate amastigote uptake**. **(A, B)** PKC

1039 typically is only slightly activated during amastigote uptake. PMA serves as a

1040 positive control. Amastigotes were added to monolayers of RAW 264.7 cells and

1041 processed as above. Shown are **(A)** representative blots demonstrating and **(B)**

1042 bar graphs quantifying relative activation of pPKC/PKC. * $P < 0.05$, *** $P < 0.001$,
1043 **** $P < 0.0001$ compared with samples indicated by brackets (ANOVA). n = 3
1044 experiments. **(C)** PMA is not toxic to amastigotes. Shown is one representative
1045 experiment of five experiments with two technical repeats following the number of
1046 amastigotes growing in DMSO-treated or PMA-treated media over 5 days relative
1047 to on day 0. ns, $P > 0.05$ compared to DMSO category by ANOVA. **(D)**
1048 Representative image demonstrating that PMA rescues trametinib inhibition of
1049 *Leishmania* amastigote uptake. BMDM were treated with DMSO, 1 μM PMA, 1
1050 μM trametinib or a combination of 1 μM trametinib and 1 μM PMA prior to
1051 incubation with IgG-opsonized amastigotes for 2 hours. **(E)** PMA increases IgG-
1052 opsonized amastigote uptake. BMDM were treated with DMSO or increasing
1053 doses of PMA (0.25, 0.5, 1, 2.5 μM) prior to incubation with IgG-opsonized
1054 amastigotes for the times indicated. n = 4 experiments. ** $P < 0.01$, *** $P < 0.001$,
1055 **** $P < 0.0001$ compared to DMSO category by ANOVA. **(F)** PMA does not
1056 affect the adhesion index for amastigotes. ns, not significant by ANOVA. **(G)**
1057 Mean PI ± SD for BMDM treated with trametinib/PMA relative to DMSO-treated
1058 samples for each experiment (100%), obtained from 3 biological experiments.
1059 **** $P < 0.0001$, ns = nonsignificant by ANOVA compared to DMSO-treated
1060 sample. **(H)** Trametinib/PMA does not affect amastigote adhesion for the
1061 experiment shown in G.
1062

1063 **Figure 4**

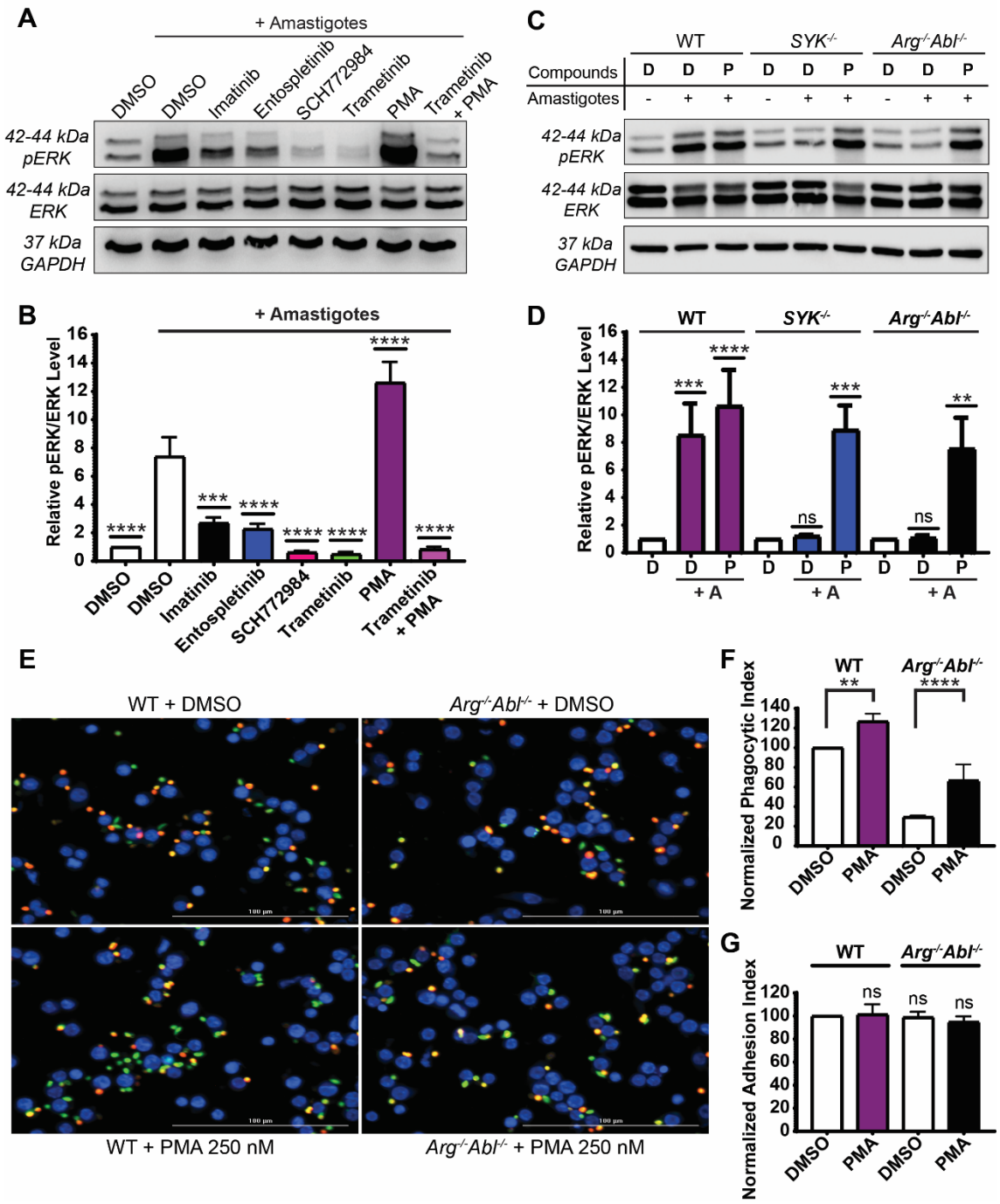

1064

1065 **Figure 4. SYK and Arg/Abl stimulate ERK1/2 phosphorylation during**

1066 **amastigote uptake. (A)** Phosphorylation of ERK1/2 in RAW 264.7 cells is

1067 induced upon amastigote uptake and is decreased by imatinib (Arg/Abl inhibitor),

1068 entospletinib (SYK inhibitor), SCH772984 (ERK1/2 inhibitor), and trametinib
1069 (MEK1/2 inhibitor). PMA serves as a positive control for pERK stimulation. RAW
1070 264.7 cells were allowed to adhere to plates, and then treated with compounds or
1071 DMSO prior to IgG-opsonized amastigote addition, lysis, and immunoblotting.
1072 Representative immunoblots of pERK1/2 (top) and total ERK1/2 (bottom) [with
1073 (+) or without (–) amastigotes] are shown. **(B)** Relative pERK levels, normalized
1074 to ERK1/2 levels, among categories shown in A. Levels of pERK are normalized
1075 to amastigote-exposed DMSO-treated RAW 264.7 cells (100%). 5 biological
1076 replicates are quantified. *** $P < 0.001$, **** $P < 0.0001$ compared with
1077 amastigote-stimulated, DMSO-treated RAW 264.7 cells (ANOVA). **(C)**
1078 Phosphorylation of ERK1/2 induced upon FcγR engagement is decreased
1079 in *SYK*$^{-/-}$ and *Arg*$^{-/-}$*Abl*$^{-/-}$ BMDM compared to WT BMDM. Shown is a
1080 representative immunoblot of pERK1/2 (top) and total ERK1/2 (bottom) in WT,
1081 *SYK*$^{-/-}$ and *Arg*$^{-/-}$*Abl*$^{-/-}$ BMDM treated with DMSO (D) or PMA (P), ± incubation
1082 with amastigotes. **(D)** Graph showing relative levels of pERK1/2, normalized to
1083 ERK1/2 levels, among WT, *SYK*$^{-/-}$, and *Arg*$^{-/-}$*Abl*$^{-/-}$ BMDM treated with DMSO
1084 (D) or PMA (P), ± amastigotes (A). ** $P < 0.01$, *** $P < 0.001$, **** $P < 0.0001$, ns:
1085 not significant by ANOVA (n = 6 experiments), compared to DMSO + amastigote
1086 category for each condition. **(E-G)** Primary cells lacking Arg and Abl exhibit
1087 decreases in amastigote uptake, but PMA can partially rescue this amastigote
1088 internalization defect. **(E)** Representative image performed as in Fig 1. **(F)** Mean
1089 phagocytic index ± SD for PMA-treated and/or *Arg*$^{-/-}$ *Abl*$^{-/-}$ BMDM relative to WT
1090 DMSO-treated BMDM. **(G)** DMSO and PMA do not affect the adhesion indexes

1091 for the experiments shown in F. n for F-G = 3 experiments. ** $P < 0.01$; *** $P <$

1092 0.001; **** $P < 0.0001$; ns, not significant compared with DMSO-treated WT

1093 BMDM (ANOVA).

1094

1095 **Figure 5**

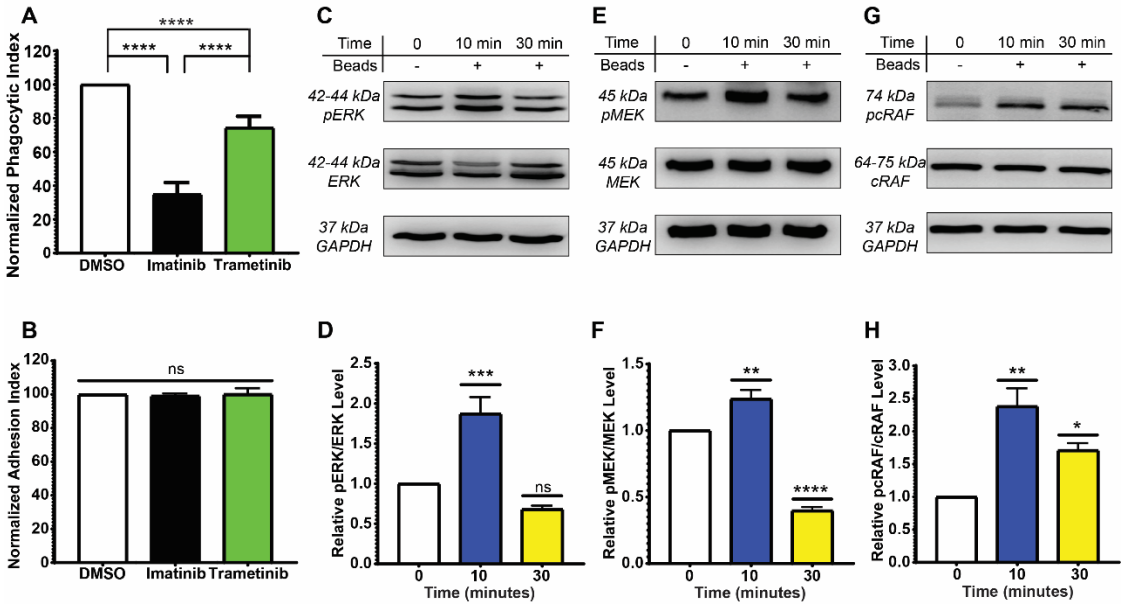

1096

1097 **Figure 5. ERK 1/2's role in *Leishmania* uptake is greater than for**

1098 **phagocytosis of beads**. **(A)** Trametinib mildly decreases bead internalization.

1099 RAW 264.7 cells were treated with 3.3 μM imatinib, 1 μM trametinib or DMSO for

1100 2 hr. prior to addition of 10 IgG-opsonized beads per RAW 264.7 cell for 2 h at

1101 37°C. Treating RAW 264.7 cells with trametinib decreases uptake of IgG-

1102 opsonized beads to a lesser degree than imatinib. Graph shows the mean PI ±

1103 SD for each category, normalized to DMSO (100%). **** $P < 0.0001$, ns: not

1104 significant compared to indicated categories by ANOVA (n = 6 biological

1105 experiments). **(B)** Imatinib and trametinib does not affect the adhesion index for

1106 beads in the experiments shown in A. **(C-H)** IgG-coated beads activate the

1107 MAPK/ERK pathway, but phosphorylation is not sustained. Beads were added to

1108 > 70% confluent RAW 264.7 cells and experiments were processed as in Fig 2.

1109 Top: Phosphorylated forms of **(C)** ERK, **(E)** MEK1/2, **(G)** cRaf and the

1110 corresponding total kinase were detected by Western blotting. Bottom: Relative

1111 activation was quantified for **(D)** ERK, **(F)** MEK1/2, and **(H)** cRaf, using the

1112 methods described in Fig 2. * $P < 0.05$, ** $P < 0.01$, *** $P < 0.001$, **** $P < 0.0001$

1113 and ns: not significant compared to 0 m timepoint by ANOVA ($n \geq 3$

1114 experiments).

1115

1116 **Figure 6**

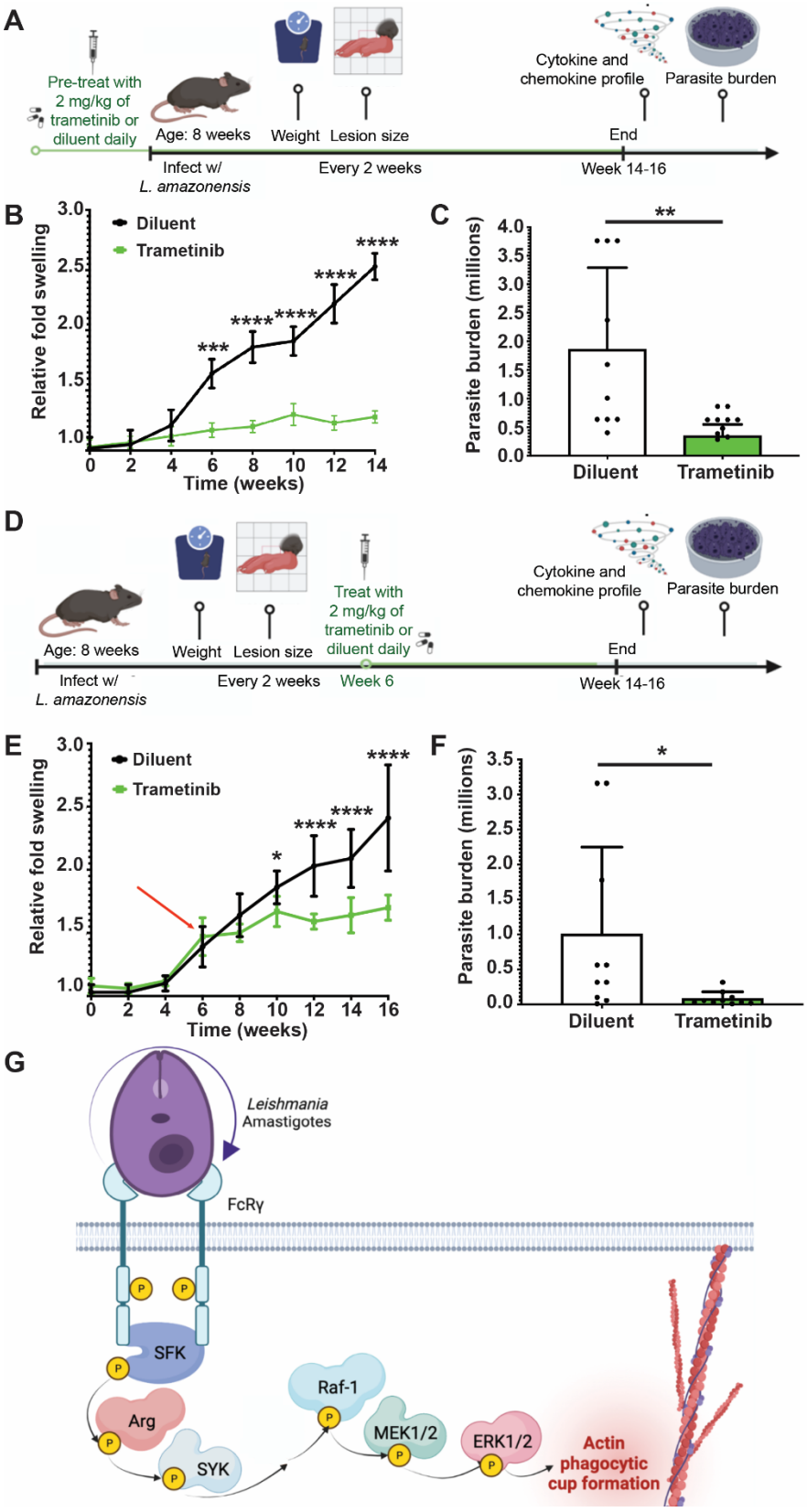

1117

1118 **Figure 6. MAPK/ERK permit efficient infection in a mouse model of**
1119 **cutaneous leishmaniasis. (A)** Mouse footpad model for cutaneous
1120 leishmaniasis. C57BL/6 mice diluent and trametinib-treated groups were injected
1121 with promastigotes in the hind footpad. Mice were given 2 mg/kg body weight of
1122 trametinib or an equal volume of diluent by oral gavage daily, starting 7 days
1123 before infection and continuing until the mice were euthanized. Two experiments
1124 were performed. Shown in the following panels is one representative experiment
1125 containing 10 female mice per group. **(B)** Trametinib given prior to infection
1126 reduces lesion size in mice. Depth of foot swelling was monitored with calipers by
1127 a blinded investigator. Results represent the mean ± SD foot size increase over
1128 the uninfected foot (normalized to 1). The control (diluent) and drug-treated
1129 groups were compared to swelling at time 0 by ANOVA; * $P < 0.05$, **** $P <$
1130 0.0001, ns, not significant. **(C)** Trametinib given prior to infection significantly
1131 reduces parasite burden. Parasite burdens in infected footpads were determined
1132 by limiting dilution as described in *Materials and Methods*. Plotted is the mean
1133 number of parasites (*i.e*, parasite burden) in millions at the end of the experiment
1134 shown in B ± SD. In this example, there were 1.41×10^6 parasites in the control
1135 mice versus 2.03×10^5 parasites in the trametinib-treated mice. *$P < 0.05$ (two-
1136 tailed *t*-test). **(D)** C57BL/6 mice diluent and trametinib-treated groups were
1137 injected with *L. amazonensis* promastigotes as above. Starting 6 weeks after
1138 inoculation (arrow), mice were given 2 mg/kg body weight of trametinib or vehicle
1139 by oral gavage daily and continuing until the experiment was terminated. **(E)**
1140 Trametinib given once lesions have begun reduces lesion size in trametinib-

1141 treated mice compared to diluent-treated mice. Arrow shows start time of drug
1142 treatment. Shown is one representative experiment containing 10 female mice
1143 per group. Statistics calculated as in B. **(F)** Lesions in mice treated with
1144 trametinib 6 weeks after infection contain fewer *Leishmania* parasites than
1145 control mice. Plotted is the mean ± SD lesion parasite burden in millions at the
1146 end of the experiment shown in E; in this example, there were 1.01 x 10^6
1147 parasites in the control mice versus 8.29 x 10^4 parasites in the trametinib-treated
1148 mice (>10-fold reduction). *P <0.05 (two-tailed t-test). (**G**) MAPK/ERK signal
1149 transduction in Mϕ facilitates *Leishmania* uptake and pathogenesis. Upon FcγR
1150 ligation by amastigotes, SFK, Arg, and SYK are activated and relay signals to the
1151 MAPK/ERK pathway, which allows the internalization of *Leishmania*. Diagrams
1152 created with Biorender.
1153

1154 **Table 1**

Experiment	Ratio	DMSO - High	Trametinib - High	DMSO - Low	Trametinib - Low
Trametinib prior to infection	**IFN Gamma/IL-4**	1.86	1.35	1.75	1.05
	IFN Gamma/IL-13	0.78	0.11	0.75	0.09
	IFN Gamma/IL-4+ IL-10+ IL-13	0.55	0.10	0.52	0.08

1155

1156 **Table 1. Ongoing trametinib treatment during *L. amazonensis* infection has**
1157 **limited effects on Th1 vs Th2 responses.** Effects of trametinib during *L.*
1158 *amazonensis* infection on cytokine secretion. Shown are profiles of draining
1159 lymph nodes isolated from diluent (DMSO) versus trametinib-treated mice treated
1160 prior to inoculation as described in methods. High refers to high stimulation with a
1161 lysate of 1 X 10^6 parasites and low refers to low stimulation with 1 X 10^5
1162 parasites. Ratios of IFNγ: IL-4, IFNγ: IL-13, and IFNγ: IL-4+10+13 were
1163 calculated from the data shown in Table 2. Trametinib may skew towards a Th2
1164 response, which should not promote lesion healing.

1165

1166 **Table 2**

Experiment	Cytokine	Treatment	Cytokine secretion (pg) after					
			Con A stimulation		High stimulation		Low treatment	
			AVG	STD	AVG	STD	AVG	STD
Trametinib prior to infection	**IFN Gamma**	DMSO	6.70	6.83	6.06	5.82	5.83	5.16
		Trametinib	0.48	0.64	0.73	1.05	0.58	0.75
		p-value	**0.01**		**0.01**		**0.005**	
	IL-1 BETA	DMSO	0.88	0.51	0.97	0.48	0.73	0.46
		Trametinib	0.45	0.12	0.42	0.11	0.39	0.09
		p-value	**0.02**		**0.002**		**0.03**	
	IL-12/IL23p40	DMSO	5.56	2.97	5.24	2.49	6.04	3.06
		Trametinib	3.28	1.18	3.39	0.79	3.53	1.31
		p-value	**0.04**		**0.04**		**0.03**	
	IL-13	DMSO	5.08	3.04	7.72	2.47	7.78	3.07
		Trametinib	7.01	2.27	6.83	1.10	6.57	1.15
		p-value	NS		NS		NS	
	IL-17A	DMSO	0.48	0.24	0.65	0.14	0.53	0.27
		Trametinib	0.59	0.09	0.74	0.25	0.53	0.25
		p-value	NS		NS		NS	
	IL-4	DMSO	2.36	1.26	3.26	1.89	3.32	2.57
		Trametinib	0.49	0.64	0.54	0.68	0.55	0.70

		p-value	**0.0006**		**0.0004**		**0.004**	
	TNF ALPHA	DMSO	2.98	1.6	2.68	2.10	2.45	1.22
		Trametinib	2.85	2.30	2.23	0.96	1.75	1.45
		p-value	NS		NS		NS	
	IL-10	DMSO	.008	.007	.02	.009	.009	.01
		Trametinib	8.94	8.78	8.36	10.44	5.16	1.06
		p-value	**0.005**		**0.02**		**0.0001**	
	MCP-1	DMSO	25.56	14.87	25.07	12.31	27.90	10.54
		Trametinib	7.23	6.43	7.23	5.87	7.23	6.56
		p-value	**0.002**		**0.0006**		**0.0001**	
	MIP-1 ALPHA	DMSO	4.69	3.95	3.93	2.77	4.62	2.96
		Trametinib	1.36	0.41	1.44	0.86	1.44	0.88
		p-value	**0.02**		**0.01**		**0.004**	

Table 2. Cytokine and chemokine profiles in diluent versus trametinib-treated, *Leishmania*-infected mice. Shown are profiles of draining lymph nodes isolated from DMSO versus trametinib mice treated prior to infection as described in methods. For high stimulation categories, a lysate containing 1 X 10^6 *L. amazonensis* was added, and for low stimulation categories, a lysate containing 1 X 10^5 parasites was added. Post 14-16 weeks, mice were sacrificed and multiplex chemokine ELISAs were performed on harvested lymph node

1175 supernatants. *P* values were determined by two-tailed *t*-tests and are listed if $P <$

1176 0.1. Bold: $P \leq 0.05$.

1177